CHALMERS
UNIVERSITY OF TECHNOLOGY

Carbon and climate efficient use of biogenic carbons in solid waste for circular chemicals through gasification

Modeling the conversion of Municipal Solid Waste (MSW) into methanol via gasification using Aspen Plus

Master's thesis in Innovative and Sustainable Chemical Engineering

MARINA MOLA MENDOZA

DEPARTMENT OF CHEMISTRY AND CHEMICAL ENGINEERING
CHALMERS UNIVERSITY OF TECHNOLOGY
Gothenburg, Sweden 2024
www.chalmers.se

Master's thesis 2024

Carbon and climate efficient use of biogenic carbons in solid waste for circular chemicals through gasification

Modeling the conversion of Municipal Solid Waste (MSW) into methanol via gasification using Aspen Plus

MARINA MOLA MENDOZA

CHALMERS
UNIVERSITY OF TECHNOLOGY

Department of Chemistry and Chemical Engineering
Chalmers University of Technology
Gothenburg, Sweden 2024

Carbon and climate efficient use of biogenic carbons in solid waste for circular chemicals through gasification
Modeling the conversion of Municipal Solid Waste (MSW) into methanol via gasification using Aspen Plus
MARINA MOLA MENDOZA

Supervisor: Sima Ajdari,RISE
Amir Soleimani Salim, RISE
Gajanan Dattarao Surywanshi, RISE
Panagiotis Evangelopoulos, RISE
Examiner: Henrik Leion, Chemistry and Chemical Engineering

Master's Thesis 2024
Department of Chemistry and Chemical Engineering
Chalmers University of Technology
SE-412 96 Gothenburg
Telephone +46 31 772 1000

Cover: Image created with DALL.E 3 representing the process of converting MSW into methanol via gasification.

Typeset in LaTeX
Printed by Chalmers Reproservice
Gothenburg, Sweden 2024

Carbon and climate efficient use of biogenic carbons in solid waste for circular chemicals through gasification
Modeling the conversion of Municipal Solid Waste (MSW) into methanol via gasification using Aspen Plus
MARINA MOLA MENDOZA
Department of Chemistry and Chemical Engineering
Chalmers University of Technology

Abstract

Municipal Solid Waste (MSW) generation is a growing global concern, aggravated by rapid urbanization, population growth, and industrialization. Annually, approximately 2.1 billion metric tons of MSW are generated, with the trend expected to rise. To address this urgent challenge, solutions must include both capacity increase and MSW treatment sustainability, like converting the non-recyclable waste into chemicals like methanol via gasification. This can potentially reduce the dependence on fossil-based raw materials in the chemical industry, increasing the circularity of the carbon in waste streams.

This study explores the feasibility of using gasification for chemical synthesis from MSW, focusing on the Bubbling Fluidized Bed (BFB) gasifier. Moreover, it includes the development of a comprehensive Aspen Plus model to simulate the MSW-to-methanol process for a feedstock input of 100 MW_{th}. It includes drying, gasification, syngas cleaning, syngas conditioning, methanol synthesis loop, and methanol purification stages. The auto-thermal gasification system is modelled using steam as gasifying agent, with a steam-to-feedstock (S/F) ratio of 0.8, and oxygen from an Air Separation Unit (ASU) to combust the volatile matter in the feedstock.

In this model, the MSW input is converted into 16.31 tonnes/h of syngas in the gasifier operating at 920 °C, requiring an oxygen flow of 2.12 kg/s from the ASU for the volatiles combustion to sustain the autothermal operation. After the cleaning stage, the syngas has an energy content of 15.31 MJ/kg on a LHV basis. Then, the ratio of H_2/CO in the syngas is adjusted to 2.5 via a Water Gas Shift reactor before entering the chemical synthesis loop. In the medium pressure vapor phase reactor, operating at 220 °C with a Cu/Zn/Al/Zr catalyst bed, the syngas is converted into methanol. After distillation, 9500 kg/h of methanol is produced with a molar purity of 99.3%. The overall process energy efficiency is 0.45 and the carbon conversion efficiency is 0.41, meaning that 41% of the biogenic carbon in the MSW is converted into the carbon contained in the methanol product.

The techno-economic analysis reveals promising financial indicators, including a payback period of 5 years, a high NPV (276.28 M€), and a competitive levelized cost of methanol of 414.92 €/tonne, suggesting that the proposed process can be economically viable and competitive with current methanol production methods.

Keywords: Municipal Solid Waste, gasification, Bubbling Fluidized Bed, Syngas, Water Gas Shift, Methanol, technoeconomic analysis.

Acknowledgements

I would like to express my gratitude to my supervisors at RISE, Amir Soleimani Salim, Sima Adjari, Gajanan Dattarao Surywanshi, and Panagiotis Evangelopoulos, for their patience, guidance and support.They provided insightful feedback and challenged me throughout this journey, and I am truly grateful for their contributions to this thesis I would also like to thank Henrik Leion, my examiner, for checking on me and being available.

Furthermore, I would like to thank the friends I made along the way in Gothenburg, you hold a special place in my heart. Thanks to Emil, for believing in my when I didn't, and pushing me when I needed it.

Y ya por último, y yo diría que más importante, a mi familia, en especial a mis padres. Todo ha sido posible gracias a vosotros, y estaré eternamente agradecida. También a mis amigos Gonzalo, Jorge, Sergio y Emilio, haceis los dias grises un poquito mejor. Ojalá daros la turra mucho más tiempo.

Millones de gracias.

Marina Mola Mendoza, Gothenburg, June 2024

List of Acronyms and Abbreviations

Below is the list of acronyms and abbreviations that have been used throughout this thesis listed in alphabetical order:

ACC	Annualized Capital Cost
AR	Air Reactor
BFB	Bubbling Fluidized Bed
BWR	Boiling Water Reactor
CAPEX	Capital Expenditure
CFB	Circulating Fluidized Bed
CEPCI	Chemical Engineering Plant Cost Index
CGC	Cold Gas Cleanup
CGE	Cold Gas Efficiency
CLG	Chemical Looping Gasification
CRF	Capital Recovery Factor
daf	dry and ash free
db	dry basis
DME	Dimethyl Ether
EIA	Energy Information Agency
ESP	Electrostatic Precipitator
FR	Fuel Reactor
GCR	Gas Cooled Reactor
GHG	Greenhouse Gases
HGC	Hot Gas Cleanup
HHV	Higher Heating Value
HTS	High-Temperature Shift
IGCC	Integrated Gasification Combined Cycle
LCA	Life Cycle Assessment

LCoM	Levelized Cost of Methanol
LHV	Lower Heating Value
LTS	Low-Temperature Shift
MDEA	Methyl Diethanol Amine
MSW	Municipal Solid Waste
NPV	Net Present Value
OC	Oxygen Carrier
OPEX	Operating Expenditure
PAHs	Polycyclic Aromatic Hydrocarbons
PBP	Payback Period
ROI	Return on Investment
RDF	Refuse Derived Fuel
R&D	Research and Development
RME	Rapeseed Methyl Ester
RWGS	Reverse Water Gas Shift
SNG	Synthetic Natural Gas
S/F	Steam-to-Feedstock ratio
TRL	Technology Readiness Level
WGS	Water Gas Shift
WtC	Waste-to-Chemicals
WtE	Waste-to-Energy
WtF	Waste-to-Fuels
WtM	Waste-to-Methanol
wb	wet basis

Contents

List of Figures

List of Tables

1
Introduction

It is estimated that 2.1 billion metric tons of municipal solid wastes (MSW) are produced yearly worldwide, and the rapid population growth, urbanization, and industrialization pose a challenge to waste management systems [11]. Additionally, unsustainable consumption patterns and increasing waste volumes can lead to improper management of this waste stream, contributing to soil, water, air pollution, and resource depletion, aggravating environmental, social, and economic problems. To address this urgent global challenge, solutions must include both capacity increase and MSW treatment sustainability, like converting the non-recyclable waste into heat, electricity, or fuels and chemicals via gasification [11].

Gasification is a thermochemical process by which carbon-containing feedstocks are converted into syngas through a series of chemical reactions at high temperatures (above 600 °C) in an oxygen-limited environment [12]. Gasification has gained increasing attention as it presents several advantages over traditional incineration technologies, like conversion into high quality syngas suitable for different applications, such as production of platform chemicals like methanol [13].

Syngas is a gaseous product mainly consisting of carbon monoxide (CO), hydrogen (H_2), carbon dioxide (CO_2), nitrogen (N_2) and light hydrocarbons like CH_4, and C_2H_4, although its composition depends on different parameters such as gasification technology, operation conditions, and feedstock characteristics [1]. Syngas is a versatile product that can be used as feedstock for chemical production and has the potential to improve the carbon neutrality and circular economy of MSW treatment. However, several challenges like feedstock variability, process optimization, and policy framework need to be addressed to ensure the viability and scalability of Waste-to-Chemicals routes for carbon-efficient waste handling.

This project aims to investigate the potential of solid waste gasification as an alternative pathway to the conventional WtE treatment, in which biogenic carbon is incinerated, to produce platform chemicals, yielding the reduction of fossil-based raw materials in the chemical industry. As the interest in sustainable solutions is

increasing, biogenic carbon in these waste streams, which make up a significant percentage, is an attractive resource that can potentially increase the circular economy and mitigate CO2 emissions, with a focus on the chemical industry. Hence, the aim is to research the carbon conversion efficiency into chemicals and its technical and economic feasibility, to analyze if this alternative is viable to reduce the reliance on fossil fuel resources and develop sustainable chemical production processes.

In addition, this project's objectives include reviewing different available gasification technologies for solid waste residues, their working principle, technical conditions, advantages, and disadvantages, along with the study of different synthesis pathways from syngas to platform chemicals. Moreover, the process with the selected combination of gasification technology and final product will be modeled in Aspen Plus, obtaining the mass and energy balances. Finally, the techno-economic feasibility of the modeled process will be assessed, providing insights into its potential for carbon-efficient waste handling. Through this assignment, the knowledge about gasification technologies and process simulation skills will be broadened.

The project is limited to the following:

- Waste as feedstock poses several challenges for gasification, given its heterogeneous nature, and chemical compositions and moisture content variations across geographical regions, and waste management systems. For this reason, an approximate composition of a typical MSW stream in Scandinavia (Norway) is chosen.

- The process modeled on Aspen Plus is to be simulated under steady-state conditions, not considering aspects like startup, shutdown, and transient states. This simplifies the modeling process while still providing insight into the overall performance and efficiency.

- The study will not focus on fuel synthesis (i.e., through Fischer-Tropsch) or hydrogen production. Instead, gasification pathways prioritizing carbon utilization, like conversion into platform chemicals, are emphasized.

- The study does not cover the current and future policy framework related to waste gasification, both national and within the EU.

The following research questions will be answered:

- What operating parameters are important to produce high quality syngas suitable for synthesis of platform chemicals?
- What is the carbon and energy efficiency of the process?
- What are the technoeconomic drivers and barriers for waste gasification into platform chemicals?

2

Background

2.1 Municipal Solid Waste (MSW)

Municipal solid waste (MSW) comprises a heterogeneous mixture of household and industry waste, including organic fractions, paper and cardboard, plastics, glass, metals, textiles, and other materials, excluding construction and demolition waste [14]. MSW composition varies significantly depending on factors like geographic location, socioeconomic factors, demographics, waste management practices, culture, and seasonal factors, as reflected in Table 2.1 [15] [16].

Table 2.1: Typical MSW composition in different countries

	Weight (%)			
Waste Fraction	**China** [17]	**Brazil** [18]	**USA** [19]	**Spain** [20]
Organic	55.59	45.3	23	49
Paper and cardboard	7.91	10.4	38.1	15
Plastics	14.1	16.8	10.5	9
Glass	-	2.7	5.5	8
Metals	-	2.3	7.8	3
Textiles, leather & rubber	7.09	5.6	6.6	5
Wood	5.82	-	5.3	2
Others	9.49	11.3	3.2	9

Waste generation tends to rise with increasing wealth, urbanization, and population, which is rapidly growing while demographics are shifting towards urban areas, accumulating more waste in cities [21]. In addition to this, the COVID-19 pandemic aggravated this situation, increasing medical and plastic packaging waste [22]. The global MSW volume is projected to continue increasing, expected to escalate from the current 2.1 billion tons to 3.4 billion tons by 2050, challenging current waste management practices and further exacerbating the climate crisis [23].

Moreover, disposal of MSW remains one of the main challenges worldwide, and solid waste management practices differ greatly among different nations [19]. For instance, disposal of MSW in landfills is still a common practice in many countries today, contributing to the contamination of groundwater and to the release of harmful emissions into the atmosphere [12]. On the other hand, waste-to-energy (WtE) technologies, like incineration, have been a promising approach for reducing MSW and recovering energy from the waste [12].
The growing concern for environmental degradation has pushed for not only quantity but also quality waste management practices. For instance, in Sweden, the ban on sorted combustible waste in landfills in 2002 and the subsequent landfill ban on organic waste in 2005 pushed for diverting MSW away from landfills [24].

According to the Energy Information Agency (EIA), on average, around fifty-six percent of MSW is classified as biogenic and, therefore, can be considered partially renewable [25]. This biogenic carbon fraction has the potential for conversion into other valuable products, like chemicals, through thermochemical processes like gasification, further reducing the dependence on fossil fuel feedstocks. The interest in waste-to-fuel and waste-to-chemical technology has increased significant, and many studies have focused on selecting the best combination of technologies and operating conditions to improve the economic feasibility of these processes.

As more countries prioritize source reduction, recycling, composting, waste-to-energy, waste-to-fuels, and waste-to-chemicals technologies, the importance of accurate data regarding the composition of the waste stream becomes of utmost importance for the success of waste management strategies [19]. MSW can be characterized into its major components and elemental composition by the proximate and ultimate analyses, respectively. The proximate analysis determines the moisture, volatile matter, fixed carbon, and ash content. On the other hand, the ultimate analysis reveals the elemental composition in terms of carbon, hydrogen, oxygen, nitrogen, sulfur, and sometimes chlorine percentages. The proximate and ultimate analyses of different MSW samples in USA, UK, and EU are reported in Table 2.2 [7] below, along with its calorific value, which is an indirect measure of how much chemical energy is converted into heat during a combustion process, reported on a high heating value basis (HHV).

Based on the data provided in Table 2.2 [7], the relatively high sulfur content in USA samples suggests potential corrosion problems during gasification processes. Moreover, the high ash content in the UK's MSW sample indicates that lower operating temperatures may be needed to prevent fouling and slagging caused by ash melting. Additionally, the high moisture content in the MSW samples in the EU

suggests the need for pre-treatment, such as drying, to enhance the gasification efficiency.

Table 2.2: Proximate analysis, Ultimate analysis, and HHV of MSW in 2018 [7]

		Element (%)		
		USA	**UK**	**EU**
Proximate	Moisture	-	-	34
	Volatile matter	91.34	51.1	-
	Ash	5.76	42.6	24
	Fixed carbon	2.9	6.3	-
Ultimate	C	51.96	35.1	25
	H	6.48	4.7	4
	O	38.55	16.1	12
	N	2.56	1.4	0.84
	S	2.57	0.2	0.13
HHV (MJ/kg)		-	15.4	9.8

2.2 Gasification

Gasification is a thermochemical process through which solid carbon-containing feedstocks, like biomass or MSW, are converted in an oxygen-controlled environment at elevated temperatures into synthesis gas (syngas), a gas mixture containing mainly hydrogen (H_2), carbon monoxide (CO), carbon dioxide (CO_2), and methane (CH_4), and other compounds including tars and char, as described in Equation 2.1. However, the syngas composition will depend on several factors like operating conditions, gasifier type, feedstock composition, residence time, and gasifying agent [1].

$$\text{MSW} \rightarrow \text{H}_2 + \text{CO} + \text{CO}_2 + \text{CH}_4 + \text{H}_2\text{O}_{(g)} + \text{tar} + \text{char} \tag{2.1}$$

Gasification encompasses different chemical reactions, mainly endothermic, for which energy is commonly supplied by oxidizing a portion of the feedstock through an allo-thermal or auto-thermal phase [5]. In the auto-thermal approach, which will be the focus of this work, internal heating of the gasifier needed to support the endothermic reactions is achieved through partial combustion, whereas in the allo-thermal approach, this energy is supplied by an external source [5]. Considering an auto-thermal system, the gasification process can be simplified into a sequence

of 4 different stages: drying, pyrolysis, oxidation, and reduction [5].

First, in the drying stage, the moisture in the feedstock is removed through evaporation. After that, in the absence of oxygen and temperatures up to 700 °C, the feedstock undergoes a thermochemical decomposition through which gaseous volatile compounds are released through chemical bond cracking, leaving char as the remaining solid fraction [5]. The pyrolysis gases can then be partially oxidized in the presence of oxygen below stoichiometric conditions, releasing the heat needed for the subsequent char gasification reactions, and sustaining the previous drying and pyrolysis stages.

In the presence of steam as a gasifying agent, the main reactions that occur are the Boudouard, char reforming, water gas shift, and methanation reactions, shown in Equations 2.2-2.5 below.

$$C + CO_2 \leftrightarrow 2CO \tag{2.2}$$

$$C + H_2O \leftrightarrow CO + H_2 \tag{2.3}$$

$$CO + H_2O \leftrightarrow CO_2 + H_2 \tag{2.4}$$

$$C + 2H_2 \leftrightarrow CH_4 \tag{2.5}$$

Furthermore, during gasification, additional reactions like tar decomposition into light hydrocarbons occur, and the equilibrium will be affected by operational parameters and initial feedstock composition, among other factors.

In this work, the purpose of generating syngas via gasification is to convert it into methanol. Therefore, selecting the most suitable gasifier type, along with additional conditioning steps and reactions, is necessary. A schematic flow diagram of the different steps involved in the production of methanol from MSW via gasification is shown in Figure 2.1. In the following sections, each step will be discussed in detail.

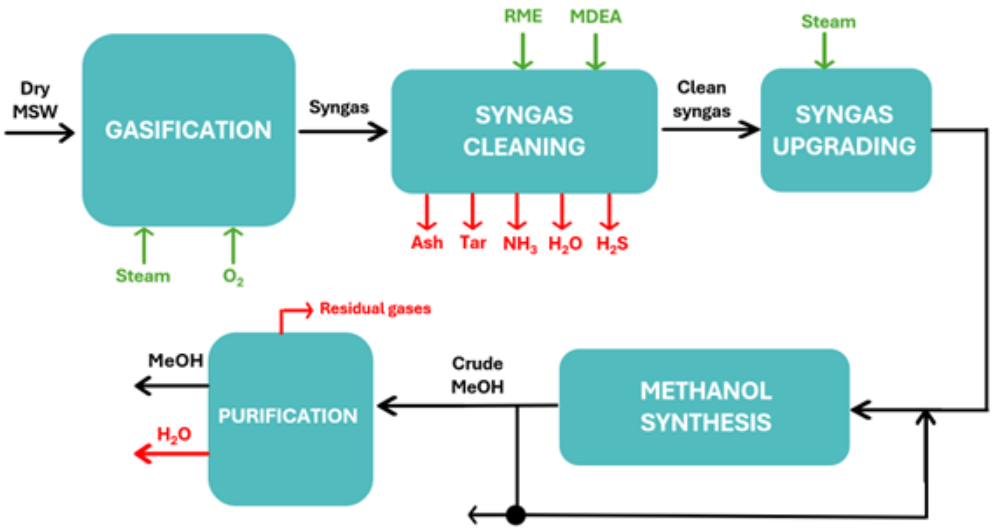

Figure 2.1: Schematic flow diagram of the process

2.3 Gasification technologies

This section aims to review different gasification technologies, including their working principle, operational constraints, and major advantages and disadvantages, all summarized in Table A.1 of Appendix A. Additionally, several commercial gasification projects spanning various feedstock types, gasifier technologies, and final products are summarized in Table A.2 of the Appendix A

2.3.1 Fixed bed gasifiers

Fixed bed reactors are one of the simplest waste gasification technologies, using diverse gasifying agents like air or steam, and operating at high temperatures ranging from 500°C to 1200 °C, high pressures between 1-100 bar for a residence time in the range of 900 to 1800 seconds [12]. Fixed bed gasifiers generally have a cylinder shape in which different zones are identified: drying, pyrolysis, gasification, and combustion [13]. The waste bed, present in an extensive section of the reactor volume, undergoes the different gasifier zones in a sequence dependent on the flow direction of both the feedstock and gasifying agent [13]. According to this flow direction criteria, two fixed bed configurations are distinguished: updraft and downdraft. Although fixed bed gasifiers offer a high carbon conversion and low ash emissions, they are not extensively deployed at large scale given the limited process flexibility and temperature control constraints [13]. Given the technologi-

cal simplicity of these reactors, the investment and operational costs are low [13].

2.3.1.1 Updraft fixed bed

In the updraft bed gasifiers, the feedstock is introduced at the top and the oxidant intake is at the bottom, creating a countercurrent flow in which the feed flows downwards, passing through the different zones depicted in Figure 2.2 [1] and syngas produced along the reactor exits at the upper section, contrary to the ash, which is deposited and collected at the bottom [1]. Since the fuel enters the drying zone first, feedstock with high moisture content can be used, while some of the resulting char is combusted in the combustion zone, providing heat [13]. This reactor is characterized by a simple construction, high thermal efficiency, and flexibility of feedstock particle size and moisture content [15]. Nevertheless, there are frequent hot spots because of temperature gradients, high amounts of tar, and low production of CO and H2 that require subsequent tart cracking treatment [13] [5].

2.3.1.2 Downdraft fixed bed

Downdraft fixed bed gasifiers operate with the fuel fed in at the top and the oxidant injected either from the top or from the sides like in Figure 2.2 [1], resulting in the movement of solids and gases in the same parallel direction. The feedstock undergoes the same zones as an updraft fixed bed gasifier but in a different sequence [13]. This reactor configuration ensures a high-quality syngas that exits at the bottom with low tar content, as some of the fuel is burnt, forming a bed of hot char through which the gases must pass [13].

The downdraft fixed bed gasifier is known for its robust and reliable technology, high carbon conversion, low tar production, and limited entrainment of ash and dust [15]. Despite its benefits, it requires a uniform feed size with low moisture content and encounters limited process flexibility and temperature control difficulties [5]. Studies have shown that downdraft fixed bed gasifiers can be used with different types of wastes, obtaining a high carbon conversion and low ash emissions [1]. However, the moisture content limits their large-scale use, posing a challenge for its use in MSW gasification [1].

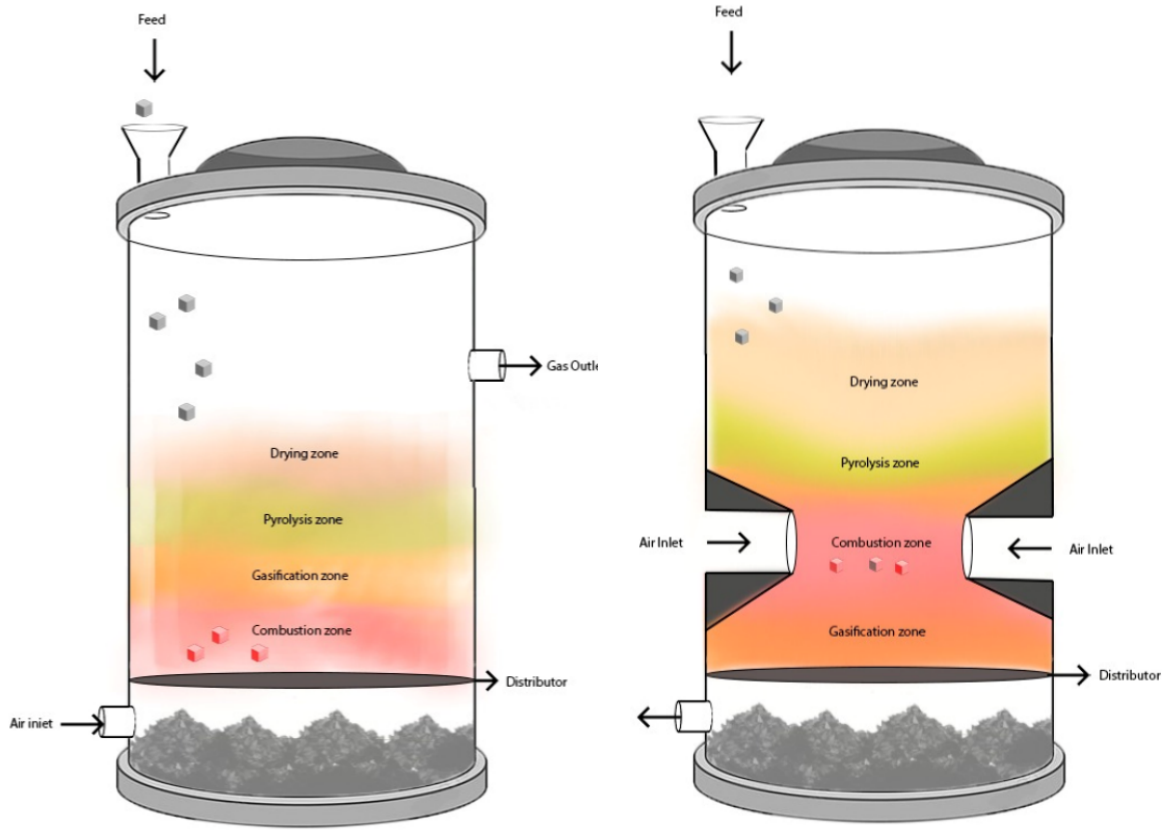

(a) (b)

Figure 2.2: Fixed bed gasifiers: (a) Updraft, (b) Downdraft [1]

2.3.2 Fluidized bed gasifiers

Fluidized bed gasifiers are a cornerstone technology in waste management and energy production, particularly for MSW gasification, since a wide variety of waste materials can be decomposed [12]. These reactors operate between 700°C and 1000°C, with the gasification agent acting as a fluidization medium injected along with small granular particles like sand, limestone, dolomite, or alumina [12] [7]. These particles increase the performance of the gasifier by promoting high heat transfer and increasing the residence time, which results in high carbon conversion rates [12]. After the gasification reactions, the syngas and solid particles are separated in a cyclone [7].

Although there are temperature limitations due to bed material agglomeration, this technology has potential selectivity for industrial applications and current re-

search favors a fluidized bed gasifier for waste and biomass gasification [26][7].

Two different fluidized bed gasifier configurations that differ in operating principle and many parameters, like the syngas composition are distinguished: bubbling fluidized bed (BFB) and circulating fluidized bed (CFB) [26].

2.3.2.1 Bubbling fluidized bed (BFB)

Bubbling fluidized bed reactors consist of a bed of inert granular material in fluidization conditions and are designed for low gas speed operating conditions between 1 and 3 m/s and temperatures spanning from 800°C to 1000°C, although temperatures below 900°C are recommended to avoid ash melting and sintering [13] [15] . The gasifying medium is injected at the bottom through a distributor plate blowing upwards, rapidly permeating the bed containing the waste and subsequent mass and heat exchange [13]. The gasification process can be divided into an initial drying and devolatilization stage, a secondary stage where volatiles and char are partially oxidized, and a final stage where char gasification and steam reforming reactions occur [2]. These stages occur mainly in the bed, but some reactions may also happen in the freeboard, the top part of the reactor through which the produced syngas exists the gasifier into the cyclone, depicted in Figure 2.3, where bed particles that are carried with the gas fall at the bottom.

This fluidized bed configuration offers several advantages, including simple construction, ease of startup, shutdown scale-up, high carbon efficiency, and lack of moving parts inside the reactor [13][15]. However, there are restrictions regarding the feed size, high investment costs, and temperature restrictions to avoid de-fluidization of the bed [5]. Nevertheless, these gasifiers have the potential for large-scale applications in sustainable waste management practices.

2.3.2.2 Circulating fluidized bed (BFB)

Circulating fluidized bed gasifiers are characterized by a significantly higher inlet velocity of the gasifying agent (3.5-5.5 $\mathrm{m} \cdot s^{-1}$) than BFB and recycle system for the bed particles [3]. The waste is fed from the side of the reactor and is rapidly heated and devolatilized before reacting with the gasification medium (steam or oxygen-enriched air) [13]. Given the higher gas speed, the solid particles are entrained in the syngas at the outlet of the reactor, and they are collected by a cyclone separator and returned to the gasifier via a downcomer [13], as shown in Figure 2.3 . The recycled solids enter the gasifier at high velocity pushing them towards

the walls and, if not operated under optimal conditions, they can accumulate and agglomerate if the moisture content is high enough [3]. Additionally, CFB gasifiers are usually operated below 900°C to avoid ash melting and slagging, like BFB [13]. Moreover, with this gasifier configuration, the residence times are short, the syngas contains low amounts of tar and increased heating value, and high carbon conversion efficiency [22]. Regardless of the advantages, it is a complex technology, difficult to control with high startup and maintenance costs and safety issues [15].

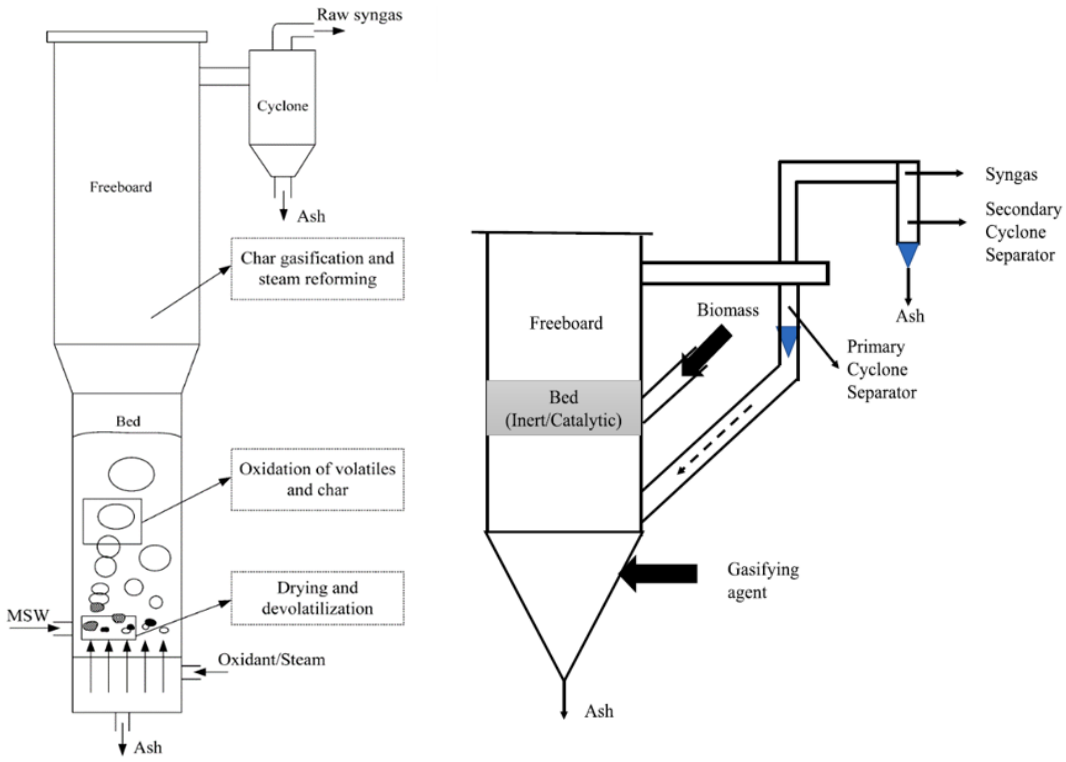

(a)[2] (b)

Figure 2.3: Fluidized bed gasifiers: (a) BFB [2], (b) CFB [3]

2.3.3 Chemical Looping Gasification (CLG)

Chemical looping gasification (CLG) of waste is a novel gasification technology for high-quality syngas production [27]. This technology consists of a fuel reactor (FR) interconnected with an air reactor (AR) through a loop seal, and an oxygen carrier (OC) that is reduced to provide oxygen for fuel conversion in the FR, and then re-oxidized in the AR to start a new cycle [4] [28]. The configuration for the CLG system is shown in Figure 2.4 [4].

Many of the reactions inside the FR are endothermic and thus demand a high energy input, while the oxidation reactions in the AR are exothermic. Therefore, the OC not only transfers oxygen between reactors but also heat through the redox reactions [28]. Given the significance of this component in the proper functioning of the system, it must provide high oxygen transport capacity, high reactivity and syngas selectivity, catalytic tar cracking capability, low costs, high mechanical strength, and high thermal stability [4]. Active transition metal oxides such as Fe_2O_3, CuO, NiO, and Mn_2O_3 are the predominant constituents of most oxygen carriers, often supported by materials like Al_2O_3, SiO_2, TiO_2, ZrO_2, bentonite, and $MgAl_2O_4$ [4]. Generally, iron-based OCs are more robust and cheaper, although their lower reactivity demands a higher oxygen carrier circulation rate [4].

Different configurations of the CLG system are possible depending on which type of reactor is used, fixed bed, BFB, or CFB, and which oxygen carrier is selected. Fixed bed reactors are not widely used because of mass and heat transfer limitations, and system complexity [28]. On the contrary, fluidized bed gasifiers are widely used for chemical looping processes given the temperature uniformity and high heat transfer[28]. Within fluidized bed reactors, different configurations of BFB-BFB, CFB-BFB, and CFB-CFB are possible, and the selection will depend on the scale and process requirements, like having enough particle circulation between reactors with limited leakage, and high temperature and pressure to achieve high efficiency [28] [29].

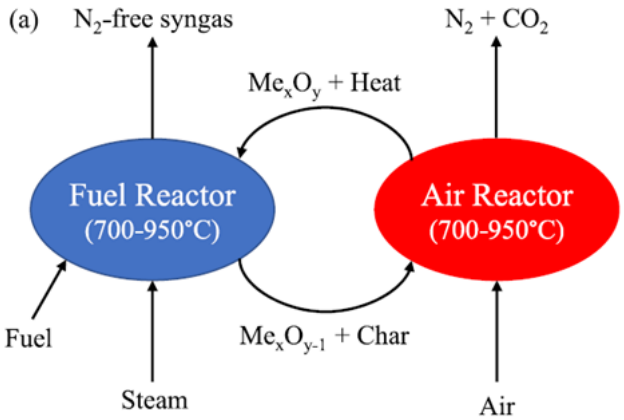

Figure 2.4: CLG system [4]

2.3.4 Entrained flow gasifiers

Entrained flow gasification technology is already available at commercial scale, mainly designed to use coal as feedstock, in various industries ranging from Integrated Gasification Combined Cycle (IGCC) plants to chemical industries [12] [26]. In this gasifier, feed fine fuel particles (0.1-1 mm) and the gasifying agent are injected in co-current [5], operating at high temperatures, typically between 1200°C and 1500°C, and high pressures, in the range of 20 to 80 bar [1]. Since the residence time of the fuel particles in the hot reaction zone is usually below 10 seconds, these particles must be small enough to achieve a high conversion, hence the need for feedstock pre-processing like grinding [26].

The feedstock can be introduced either dry, using a pneumatic feeding system that injects it as pressurized powder solid fuel, or as a water slurry, atomized and fed as pulverized solid fuel [5]. Although water acts as a transport medium and temperature moderator [13], the thermal energy needed to heat up and evaporate the slurry suggests that dry-fed systems are potentially more efficient [26]. Additionally, two operational settings are distinguished based on the operating temperature: slagging and non-slagging. In a slagging reactor the ash leaves as liquid slag, while in a non-slagging reactor, the walls are slag-free [26]. Figure 2.5 [1] shows a schematic configuration of a slagging entrained flow gasifier, where a turbulent flame at the top combusts some of the fed fuel, providing high amounts of heat at a higher temperature than the ash melting point. This high temperature yields high-quality syngas, and the melted ash is discharged as molten slag into the quench chamber for cooling, encapsulating metals [13].

Adapting this gasification technology to other feedstocks like biomass or waste faces several challenges, like fuel pretreatment and ash composition and behavior, thus still under development [26]. When entrained flow gasifiers are used for waste or biomass gasification, a torrefaction-based pretreatment is required to meet the moisture content and bulk density limitations of this reactor [5]. Torrefaction is a thermochemical process by which the feedstock is heated under inert conditions, resulting in a solid product with lower moisture content, higher heating value, more uniform properties, and lower bulk density, and in a mixture of condensable and non-condensable gases [30]. Additionally, other pretreatments like Hydrothermal Carbonization (HTC) can be used to improve the feedstock grindability [26].

On the one hand, this technology achieves low concentration of tar in the syngas, and high carbon conversion at short residence time, without process control problems. On the contrary, the challenges attributed to waste and biomass feedstocks, like preprocessing and pretreatment, translate into higher operational and main-

tenance costs [5].

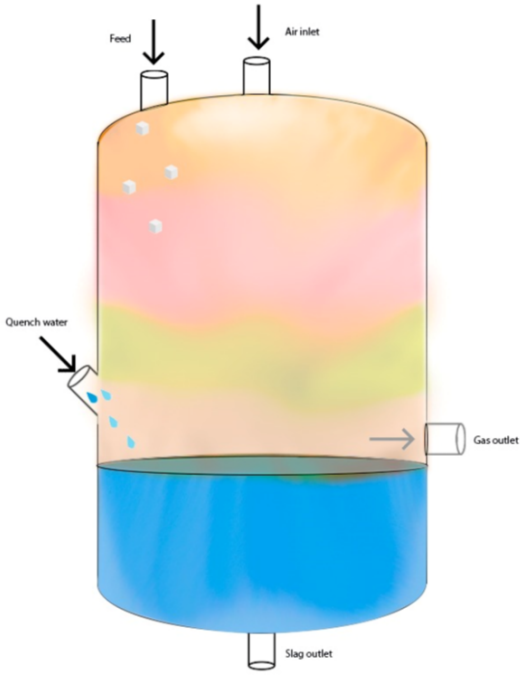

Figure 2.5: Entrained flow gasifier [1]

2.3.5 Plasma gasifiers

Plasma gasification is a fairly new technology that breaks down waste into clean syngas by using an ionized gas stream at approximately 10000 ◦ C, obtained through plasma torches by electric discharge, referred to as "arc", and a gasification medium (air, O_2, or steam), operating between 1 and 3 bar [1][15] [5]. The waste is introduced at the top of the reactor, while the gasifying agent enters at the side, as shown in Figure 2.6 [5]. The plasma torches are the heat source that provides the high-temperature environment needed to convert the organic material in the feedstock into syngas, which exits at the top, and the inorganic fraction into inert and vitrified slag, which exists at the bottom and can be further treated to use it in construction applications [12][15].
Contrary to other gasification technologies, there are no limitations regarding feedstock moisture content, and feedstock particle size is flexible, making waste pretreatment and preprocessing unnecessary [1]. Although the high operational temperatures allow for high conversion efficiency and minimal pollutant emissions,

they also contribute to high operational costs given the substantial electricity demand of these gasifiers, ranging from 1200 to 2500 MJ per ton of MSW, limiting its commercial viability in large-scale [12]. Moreover, there are some security concerns and high maintenance costs associated with the replacement of the electrodes in the plasma torches [15]. Despite these techno-economical constraints, several small- scale plants have been established, and this technology is interesting for hazardous waste, like that produced by health care facilities [7].

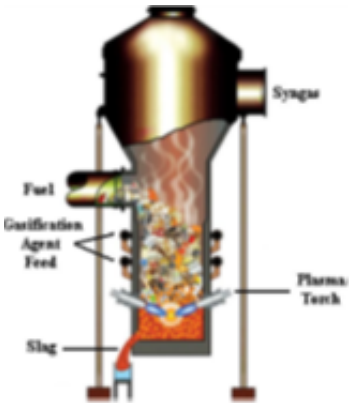

Figure 2.6: Plasma gasification technology [5]

2.3.6 Rotary kiln gasifiers

Rotary kilns are a mature technology deployed in several industrial applications, like waste incineration and RDF and biomass gasification, consisting of a slightly tilted (1-3%) cylindrical steel chamber lined with abrasion-resistant refractory to prevent overheating that slowly rotates around its axis (approximately 1.5 rpm) [13] [5]. This rotation moves solids into and out of the high-temperature reaction zone and exposes new solid surfaces to the gasification agent, improving the gas-solid contact [13] [5]. Despite this, the heat and mass transfer between gas and solid is very effective, needing high residence times in the range of hours for high conversion [5].

The most common configuration for a rotary kiln is countercurrent with the feedstock introduced at the top of the reactor and the gasification agents injected at the exit end of the kiln, as shown in Figure 2.7 [5], and operates at a range of temperatures between 300°C and 600°C [1]. The rotary kiln design ensures temperature uniformity in the radial direction, which avoids slagging [31].

While rotary kilns offer high flexibility, conversion rates, simple construction, and low sensitivity towards feedstock characteristics like moisture content and particle size, they also present challenges like high tar production, and maintenance costs [15]. Despite these challenges, rotary kilns have been proven successful in the thermal conversion of various wastes, including plastics [31].

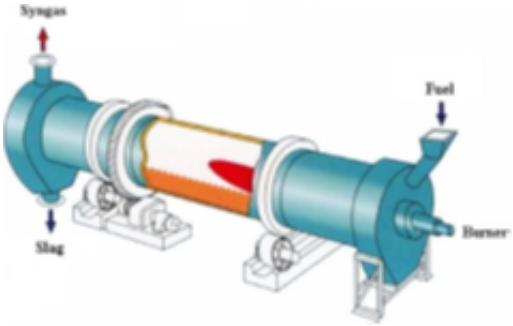

Figure 2.7: Rotary kiln gasifier [5]

Gasification techonolgy selection

Fluidized bed reactors pose characteristics that make them suitable to overcome the challenges faced by the other technologies mentioned above, like feedstock composition and size flexibility, rapid heating, and consistent operation at high temperatures [1]. The fluidization mechanism enhances mass and heat transfer, ensuring a uniform temperature distribution across the gasifier cross-section, ultimately yielding higher syngas production than, for example, fixed bed gasifiers [1]. Additionally, when compared to other gasifiers, fluidized bed reactors have lower capital cost per ton of landfilled MSW [1].
Fluidized bed gasifiers stand out as the preferred choice for waste gasification, supported by their technological maturity and success in numerous commercial large-scale projects compiled in Table 2. Among fluidized bed gasifiers, bubbling fluidized bed (BFB) ones have lower investment and maintenance costs than the circulating fluidized bed (CFB) because their operation and construction are simpler, without diminishing their efficiency in producing high-quality syngas [1].

Therefore, BFB gasifiers are the preferred and frequently chosen technology for waste conversion and will be the selected technology for this project.

2.4 Syngas upgrading

Syngas has widely been utilized for energy and power applications. In recent years, efforts have been redirected towards syngas transformation into valuable fuels, such as hydrogen or biodiesel, contributing to sustainable energy solutions. However, this work focuses on waste-to-chemical conversion, aimed to recycle biogenic carbon to mitigate environmental impacts derived from the chemical industry. With that purpose, several chemicals have been evaluated, alongside synthetic natural gas (SNG) for comparison, and the operational conditions, catalysts, pricing, and the technology readiness level (TRL) of each process is compiled in Table A.3 in Appendix A
.
Additionally, different commercial projects worldwide, detailing the feedstock type, end-product, and current status are summarized in Table A.4 in Appendix A
.
Methanol synthesis from waste-derived syngas involves the water gas shift reaction, converting the CO and H_2 mixture into methanol, typically over well-established and robust $Cu/ZnO/Al_2O_3$ oxide catalysts. Ethanol and DME synthesis require additional steps once methanol has been produced, like methanol dehydration, therefore impacting overall process efficiency and costs. In addition to this, DME often requires the use of complex catalysts like zeolites.

Moreover, Waste to Methanol processes have been extensively used in commercial-scale projects, as reported in Table 4, holding an advantage in terms of TRL compared to the other chemicals. Biomethane, while promising, faces many difficulties related to cost-effectiveness since natural gas from non-renewable sources is significantly cheaper, reflecting that further technology and process improvements are required. Therefore, methanol is the preferred and frequently chosen platform chemical to synthesize from waste-derived syngas and will be the selected product for this project.

2.5 Syngas cleaning

In gasification processes different undesired species are formed, like particulate matter, tar, sulfur, and nitrogen compounds. The extent to which these impurities form mainly depends on the feedstock used, the gasifier type, and the operating conditions. For instance, biomass gasification generates large amounts of particulate matter and sulfur compounds, while gasification of waste plastic feedstocks generates larger amounts of tars and significantly lower concentrations of sulfur

compounds (often not detectable) [32]. These impurities hinder product yields, affect the overall efficiency of the process, increase the costs, and given their harmful pollutant nature, increase the environmental negative impact if released, hence the importance of the syngas cleaning stage.

Additionally, the downstream gas-phase methanol synthesis process contains a copper-based catalyst that is easily poisoned by the contaminants in the syngas produced from waste streams in the gasification process, requiring a multi-step purification [33]. Table 2.3 shows the maximum allowable amount of each contaminant in the syngas feed suitable for the downstream methanol synthesis unit.

Table 2.3: Syngas cleaning requirements for methanol synthesis

Contaminant	**Value (mg/m^3)**
Particulate matter (ash, dust, char)	<0.02
Tars	<0.1
Sulfur (H_2, COS)	<0.01–1
Nitrogen (NH_3, HCN)	<0.1
Alkali	n.a^*
Halides (HCl)	<0.1

There are different methods for syngas cleaning, and depending on where they are applied, they can be classified into primary or secondary methods. Primary methods, often called 'in-situ' methods, are implemented within the gasifier via specialized design techniques (selection of the gasifier type, gasifying agent) and precise control of the reactor's operational parameters, like temperature, equivalence ratio, residence time, and addition of active bed materials like CaO or dolomite [34]. On the other hand, secondary methods are implemented in downstream processes, do not interfere with the gasification process, and can be classified into Cold Gas Cleanup (CGC) or Hot Gas Cleanup (HGC).

Cold gas cleanup (CGC) processes are commonly recognized as the conventional approach for their effectiveness in removing contaminants from syngas streams [32]. Typically conducted at low temperatures, as high as 100 °C, and often at or below room temperature, CGC utilizes either wet or dry processes [35]. Wet CGC processes employ liquid absorbents and are frequently employed due to their ability to remove multiple contaminants such as NH_3, HCl, and H_2S [36]. CGC techniques are relevant due to their proven high efficiency in multiple contaminant removal and reliability [36]. However, the main disadvantages are associated with the need for syngas cooling, which incurs an energy penalty on plant efficiency,

and the disposal of contaminant streams, which translates into additional costs to meet environmental standards [32].

On the other hand, HGC processes are usually operated above 200 °C, which is thermodynamically favorable for many syngas applications [35]. This approach reduces waste streams and achieves a better syngas conversion with fewer byproducts. Contrary to CGC, the sensible and latent heat is not wasted, increasing the overall efficiency [34]. Moreover, ongoing research into catalysts for HGC aims to optimize contaminant removal, potentially converting them into useful products and enhance overall process efficiency [36].

2.5.1 Particulate matter

Particulate matter in syngas, ranging in size from µm to mm, comprises mainly inorganic compounds and residual solid carbon originating from the gasification process, and its composition mainly depends on the feedstock used. The inorganic fraction includes alkali metals like potassium and sodium, silica, and other trace metals, usually from bed material or catalysts [35].

The removal of these flying particles, classified according to their aerodynamic diameter (PM_{10} denotes particles smaller than 10 µm), is essential to avoid fouling, corrosion, and erosion problems that hinder the efficiency and safety of the process. Often, removal efficiencies greater than 99% are required and, typically, particles of a certain size are removed to keep them below a specific level, like removing PM_5 below 0.02 mg/m^3 for methanol synthesis [32].

Among particulate matter removal technologies, cyclones are one of the most widely used devices for solids separation, which use centripetal acceleration to separate the solid particles from the vapors by inertial forces, operating at temperatures that can exceed 1000°C and achieving removal efficiencies of more than 99,6% [35]. However, multiple cyclones might be needed if finer particles need to be removed, making it unattractive for large-scale projects with high syngas volumes. Barrier filtration methods, like fabric filters and rigid ceramic or metallic filters, effectively remove particles larger than 1mm and smaller than 100 µm, with removal rates up to 99,99%, limited by temperatures up to 400°C [35]. Moreover, electrostatic precipitators (ESP) exploit electric fields to charge fine particles, removing them from the gas stream with a force more than 100 times stronger than gravity, although their application is restricted in high-temperature settings because of the temperature effects on properties like density, viscosity and resistivity which are crucial for ESP functionality [35].

Additionally, wet scrubbers employing water as a scrubbing agent and operating near ambient temperatures are predominantly used in CGC processes and are characterized by spray, wet dynamic, cyclonic spray, Venturi, and electrostatic technologies, providing increasing efficiency for submicron particulate matter [32][35].

2.5.2 Tar

Tar in syngas, often defined as any hydrocarbon with a higher molecular weight than benzene (78 g/mol), comprises condensable organic compounds ranging from primary oxygenated products to heavier deoxygenated hydrocarbons and polycyclic aromatic hydrocarbons (PAHs), which are grouped into classes [35]. Class 2 tars are composed of heterocyclic components like phenol and are water-soluble. Class 3 tars comprise light aromatic components, while Class 4 tars consist of light polyaromatic hydrocarbons (2-3 rings) that condense at moderate concentrations and intermediate temperatures, and Class 5 tars encompass heavy polyaromatic hydrocarbons (4-5 rings) condensing at higher temperatures but lower concentrations [37]. These compounds are formed during thermochemical conversion processes, and their concentration in syngas varies depending on operating conditions like temperature, pressure, feedstock composition, and residence time [35] [36]. The tar composition of the MILENA lab scale indirect gasifier based on beech wood as feedstock is shown in Table 2.4 [37].

Tars condense in the low-temperature zone of downstream applications, which poses a challenge in gasification due to their potential to foul equipment, corrode pipelines, block filters, and deactivate catalysts [34]. Therefore, the removal of these compounds is essential to prevent efficiency losses and ensure the proper functioning of downstream applications.

Despite efforts to define and measure tar, its complex chemical nature poses challenges in collection and analysis [32] [35]. However, controlling operating conditions and employing suitable gas-cleaning systems can help mitigate tar-related issues. Additionally, while complete elimination of tar is preferable, another approach involves removing enough tar to ensure its dew point remains below the lowest temperature encountered by the gas stream [35].

Tar can be removed by inertial separation devices operating at temperatures below 450°C when tar condensation into fine aerosols within the syngas begins. These aerosols resemble particulate matter since they are significantly heavier than the vapors, which makes them suitable for removal with cyclones, filters, or ESP [35].

Table 2.4: MILENA lab scale tar concentration normalized to 0% N_2

	Temperature (°C)					
Tars (mg/m^3_{dry})	**776**	**782**	**832**	**861**	**880**	**882**
Class 2	4795	4279	2057	1118	1013	504
Class 3	217	301	262	311	203	164
Class 4	8737	9980	12496	145676	11771	2374
Class 5	1131	1417	2075	3356	2216	2374

Sand bed filters, along with activated carbon filters known for their high porosity, are effective filters for tar removal, achieving reduction levels ranging from 50% to 97% in biomass-derived syngas [32].

More prominently used are the wet scrubbers, which effectively remove tar based on absorption mechanisms. Although tar is non-soluble in water, in water-based scrubbers like those used in the Harboøre updraft gasification plant, the gas temperature lowers enough for these compounds to form aerosols, easily absorbed into water droplets, which are then separated in a settling tank, recirculating the water back to the process [32][35].

Recent advancements have focused on oil-based absorbents because of their overall higher efficiencies and the regeneration potential with hot air stripping, like the oil-based multistage OLGA scrubber developed by the Energy Research Centre of the Netherlands (ECN) [32]. Similarly, the RME scrubber technology, demonstrated at the Güssing biomass DFB gasification plant and GoBiGas demonstration plant, utilizes rapeseed oil methyl esters to effectively remove tar, ammonia, and acidic components from syngas streams [32] [38]. However, this oil-based approach is economically feasible only in large-scale installations, given the process complexity and cost of the absorbents [36].

2.5.3 Sulfur compounds

Sulfur-containing species in the syngas primarily comprise hydrogen sulfide (H_2S) and lesser amounts of carbonyl sulfide (COS), and their concentration typically ranges from 100 to 1000 parts per million (ppm), depending on the feedstock, gasification technology, and operating parameters [34] [39]. For instance, biomass sulfur content is between 0.1-0.5 g/kg, while in waste plastic feedstocks, it is around 0.03 wt.% dry basis and sometimes not even detectable [32].

These sulfur compounds pose significant challenges as they corrode metal surfaces, have a high environmental impact, and poison catalysts utilized in syngas cleaning and downstream processes [32]. Thus, the removal of sulfur to parts per billion levels is often necessary to mitigate these detrimental effects [35]. Various gas cleanup technologies, including both dry and liquid-based chemical and physical processes covering a wide temperature range, have been developed for sulfur removal and mitigation of other acid gases, which includes CO_2 [35].

In-situ methods incorporate calcium-based sorbents like dolomite directly into the gasifier bed, facilitating the conversion of sulfur compounds [32]. On the other hand, downstream removal techniques employ adsorption and absorption processes. Adsorption, widely employed in HGC, relies on materials like metal oxides or porous sorbents like activated carbon, to which gaseous sulfur species bind either physically or chemically [13] [36]. Copper and zinc oxides are abundant and have reported removal efficiencies surpassing 99%, achieving H2S concentrations lower than 100 ppmv, although their regeneration is crucial to reduce waste streams and material inputs [13][32].

For wet gas cleanup, either chemical or physical absorption is most often employed [35]. In the chemical absorption process, acid gas components react with the solvent molecules, leading to their dissolution within the solvent, which is then regenerated in a stripper and recycled back [35] [40]. This process commonly relies on amine-based solvents like monoethanolamine (MEA), di-ethanolamine (DEA), and the preferred methyl-diethanolamine (MDEA) [36] [40]. Conversely, in physical absorption, the syngas sulfur components are absorbed directly into the solvent molecule, using absorbents like di-methyl-ethers of polyethylene glycol (Selexol process) or chilled methanol (Rectisol process) [40]. This method is preferred for fuel synthesis, since concentrations below 1 ppmv can be achieved to prevent downstream catalyst poisoning, while chemical absorption with MDEA is used when less stringent sulfur requirements need to be met.

2.5.4 Nitrogen compounds

Nitrogen-containing compounds in the syngas primarily comprise ammonia (NH_3), and lesser amounts of hydrogen cyanide (HCN). Ammonia is the predominant contaminant with a concentration ranging from a hundred to a few thousand ppm, depending on feedstock type, gasifier type, and process conditions like temperature and residence time [32]. Although a significant portion of ammonia decomposes to molecular nitrogen (N_2) at typical gasification temperatures, even low levels of ammonia can pose challenges like catalyst deactivation in certain syngas upgrad-

ing applications [35].

Due to the high solubility of NH_3 and HCN in water, water-based scrubbing is regarded as the conventional approach for cold gas removal of nitrogen-containing contaminants since ammonia concentrations are reduced with more than 99% efficiency [36]. Furthermore, it often carried out simultaneously with tar removal [36]. For instance, the condensate obtained during tar scrubbing with RME at 50°C removed ammonia at 30%-50% efficiency depending on the initial concentration [35]. Furthermore, the use of dilute acid absorbents has emerged as an advancement over traditional water-based scrubbing, which additionally have the potential to co-absorb acid gases like H_2S [36].

2.6 Syngas conditioning

To produce methanol directly from syngas, the H_2/CO ratio in the syngas must be approximately 2.4-2.5, and the CO_2/CO ratio preferably around 0.13-0.14 [41]. However, the syngas composition depends on the feedstock used, and the required ratios are hard to obtain directly from the gasification unit, hence the need to add a syngas conditioning step to shift the ratios towards the optimal ones before the synthesis. For example, syngas produced from natural gas reforming is too rich in hydrogen, while the one produced from biomass is hydrogen deficient, both needing composition adjustments [42].

2.6.1 Water Gas Shift (WGS)

The most common method to adjust the H_2/CO ratio is by using a WGS reactor, in which the exothermic and reversible reaction in Equation 2.6 [43] takes place.

$$CO_{(g)} + H_2O_{(g)} \rightleftharpoons CO_{2(g)} + H_{2(g)} \quad \Delta H_{298K} = -41.15 \text{ kJ/mol} \tag{2.6}$$

The water-gas shift (WGS) process typically employs two separate reactors due to thermodynamic limitations: a high-temperature shift reactor (HTS) and a low-temperature shift reactor (LTS) connected by a heat exchanger.

Based on the equilibrium reaction and Le Châtelier's principle, in the first reactor, typically operated between 310-450 °C and 25–35 bar, kinetics is favored due to high temperature, while thermodynamics is favored in the low-temperature reactor, usually operated at 200-240 °C, all of which allow to obtain high hydrogen

yields [44].

This method is temperature sensitive since it governs the direction of the WGS reaction. Conversely, given that it is an exothermic reaction and there is no mole number variation, operating pressure has almost no influence in the process [45].

Moreover, for chemical downstream applications, the water gas shift reaction is required after the syngas cleaning step, also known as sweet gas shift [40].

2.7 Methanol synthesis

Methanol is synthesized from syngas via CO and CO_2 hydrogenation, both exothermic and reversible reactions in Equation 2.7 [46] and Equation 2.8 [46], respectively, while the slightly endothermic reverse WGS reaction in Equation 2.9 [46] occurs in parallel and is favored by increased CO_2 partial pressure in the syngas [47].

$$CO_{(g)} + {}_2H_{2(g)} \rightleftharpoons CH_3OH_{(l)} \quad \Delta H_{298K} = -90.77 \text{ kJ/mol} \tag{2.7}$$

$$CO_{2(g)} + {}_3H_{2(g)} \rightleftharpoons CH_3OH_{(L)} + H_2O_{(g)} \quad \Delta H_{298K} = -49.16 \text{ kJ/mol} \tag{2.8}$$

$$CO_{2(g)} + H_{2(g)} \rightleftharpoons CO_{(g)} + H_2O_{(g)} \quad \Delta H_{298K} = 41.21 \text{ kJ/mol} \tag{2.9}$$

Hydrogenation reactions reduce the number of moles [24], translating into a decrease in the total gas volume that will affect the equilibrium. According to Le Châtelier's principle, for exothermic reactions, an increase in temperature will shift the equilibrium in the endothermic direction that consumes heat. Conversely, an increase in temperature in an endothermic reaction will shift the equilibrium in the exothermic direction. Because of this, high methanol conversion is achieved at low temperatures and high pressures, promoting the exothermic direction in the hydrogenation reactions and lowering the extent of the reverse WGS.

However, a compromise between reaction rate and catalyst activity must be reached. On one hand, temperatures below 200°C are insufficient to achieve significant reaction rates on state-of-the-art catalysts [47]. On the other hand, operating temperatures beyond 300 °C promote catalyst deactivation, sintering and fusion problems, likely resulting in irreversible damage to the catalyst [48]. Therefore, methanol synthesis is typically carried out in the ranges of 220-280 °C and pressures between 50 and 100 bar [47].

Moreover, syngas can also undergo other reactions resulting in the formation of additional hydrocarbons like methane, ethanol, or more complex hydrocarbons

[49]. The selectivity and efficiency of the catalyst significantly impact the overall conversion efficiency and will play a significant role in avoiding undesired products [49]. Copper-based catalysts have been extensively used for several decades and continue to spark research interest due to their remarkable catalytic properties. The highest active and selective commercial catalysts are commonly based on $Cu/ZnO/Al_2O_3$, and although the composition varies, Cu typically ranges between 20-80%, ZnO between 15-50%, and Al_2O_3 between 4-30% [46]. The addition of oxides like Al_2O_3 or ZrO_2 has proved to increase the dispersion of copper particles in the catalyst, whereas the addition of Ga_2O_3 or Cr_2O_3 increases the activity per unit copper surface area of the catalyst [50]. Moreover, the Cu/ZnO multicomponent catalyst with $ZrO_2/Al_2O_3/SiO_2$ additions has been successfully used for methanol synthesis operation in a bench plant, found to have great stability during long-term methanol and achieve high methanol purities [50].

Additionally, to improve the methanol conversion in conventional gas phase reactors, in which one pass of reactant gas has 16-20% CO conversion, unreacted syngas can be recycled after product separation by condensation, achieving an 80-100% conversion [46] [48] [51].
A schematic methanol synthesis process from syngas is shown in Figure 2.8. Since the outlet stream from the reactor is in gaseous form, the mixture undergoes cooling before the recycle stream is separated, typically in a gas-liquid flash separator [52]. To avoid the accumulation of undesired components in the pipes and in the reactor, a small amount of the unreacted syngas will be purged, while the crude methanol (mixture of methanol and water) will be sent to a purification stage, typically one or two distillation columns, to obtain methanol according to the commercial quality standards. During distillation, incondensable gases like H_2, CO, and CO_2, as well as water, are separated from methanol. The major drawback of this method is that it is very energy intensive and inefficient regarding cost savings, prompting ongoing efforts towards finding a cost-effective alternative for methanol-water mixtures [53].

2.7.1 Methanol production technologies

In this work, methanol synthesis will be carried out in the gas phase. Reactor types are commonly categorized based on operating conditions into adiabatic and isothermal reactors depending on how heat is removed from the system to maximize methanol conversion.

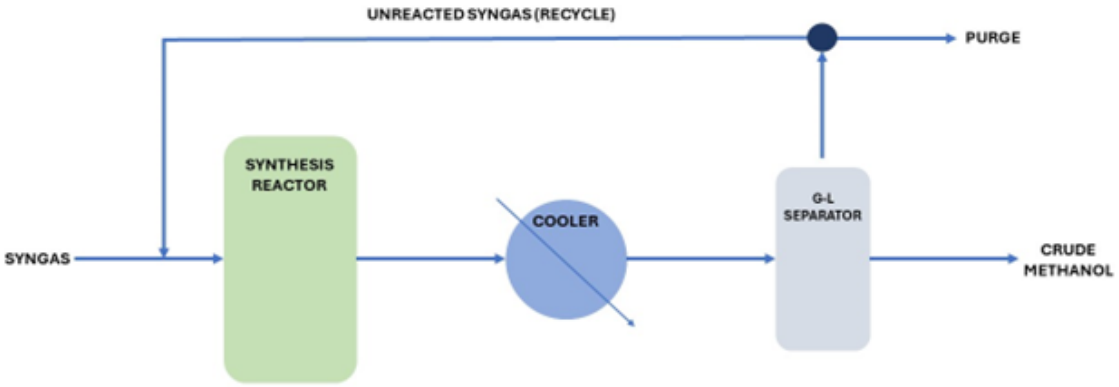

Figure 2.8: Schematic methanol synthesis configuration

2.7.1.1 Adiabatic reactors

In adiabatic systems, the syngas flows through multiple catalytic packed-bed reactors arranged sequentially, and the generated heat is removed by intermediate heat exchangers [46].

One of the main disadvantages of this system is the high equilibrium temperatures developed within the reaction zone, translating into low conversions for each pass, a high recycle ratio and ultimately decreasing the catalyst activity and lifetime due to sintering and fusion [46] [6]. On the other hand, the installation costs are generally low, and the production capacity is high [6]. Moreover, adiabatic reactors with axial flow have a simple design but high material costs given the large pressure drop and vessel diameter [46]. Conversely, adiabatic reactors with radial flow, while having lower pressure drops, are more complex and expensive reactor structures [46]. Additionally, two sub-configurations of the adiabatic reactors are found: indirect cooled reactor, and quench reactor.

The indirectly cooled reactor is a simple and common system used for methanol production from syngas, consisting of a series of adiabatic reactors connected by a series of external coolers that lower the process stream's temperature to achieve very high productivity [6]. The schematic configuration of this reactor, along with the reaction path, is shown in Figure 2.9.

One of the simplest designs is the quench reactor, in which only a fraction of the syngas is preheated and fed on top of the reactor, increasing the reactor's temperature as the reactants are converted [6]. The rest of the syngas is fed cold at different injection points along the catalytic reactor volume, lowering the temper-

ature and increasing the syngas conversion. One of the main disadvantages of this configuration is that only the preheated syngas fed at the top is processed by the total catalytic volume while the rest fed stepwise along the reactor, is only exposed to a fraction of it [6]. The schematic configuration of this reactor, along with the reaction path, is shown in Figure 2.10.

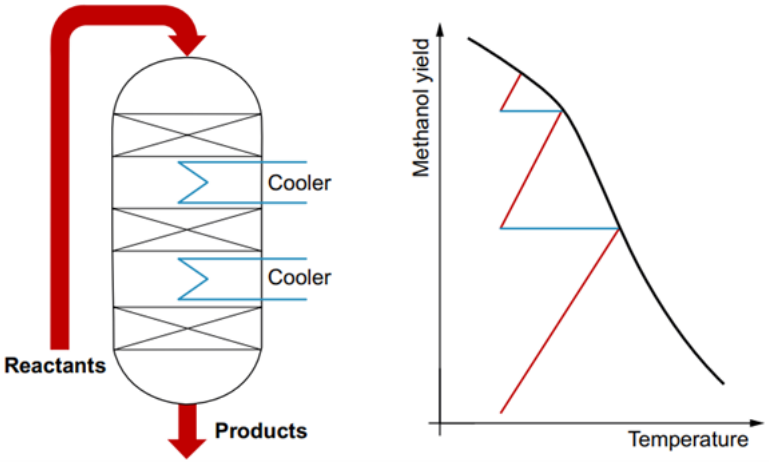

Figure 2.9: Indirect cooled reactor [6]

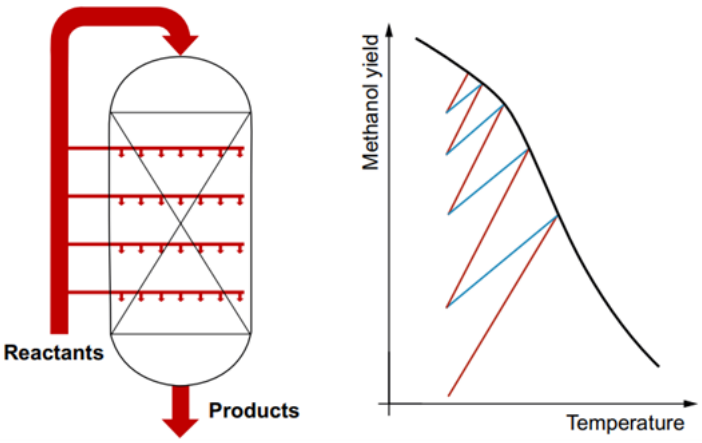

Figure 2.10: Quench reactor [6]

2.7.1.2 Isothermal reactors

In isothermal systems, continuous cooling is supplied either through water or gas so that the temperature is kept constant, preferably between 240 °C and 260 °C to achieve a balance between successful reaction rates and thermodynamically favorable equilibrium conditions [6].

Depending on the cooling agent, there are two reactor categories: gas-cooled reactor (GCR) and boiling water reactor (BWR) [46]. Additionally, for the BWR, two sub-configurations exist depending on where the boiling water flows through. The catalyst can be packed inside the tubes, with the syngas flowing axially through them and the boiling water flowing between the tubes (shell), or it can be packed between the tubes, with the syngas flowing either axially or radially through the shell and the boiling water flowing through the tubes [33][46]. An example of the first sub-configuration widely used in the industry is the Lurgi (now Air Liquide) methanol reactor, in which the boiling water flowing through the shell removes the heat released in the reactions occurring inside the tubes, where the catalyst is loaded [54]. The schematic configuration of a typical BWR reactor, along with the reaction path, is shown in Figure 2.11.

The main highlights of these reactors include high methanol conversion rates, uniform temperatures with minimal fluctuations that hinder undesired side reactions, optimal temperature control that prolongs the catalyst lifetime by avoiding sintering or deactivation, which translates into lower catalyst volumes, and high heat transfer efficiency [33] [6] [54]. Moreover, the heat released during the methanol synthesis, in the form of saturated medium-pressure steam, can be efficiently recovered and utilized in the subsequent methanol purification process as a heat source in the distillation column, contributing to the process's overall efficiency [33]. However, given the complexity of the reactor structures, the capital costs are very elevated, and the production scale limited because of the tube bundle [33] [6] [54].

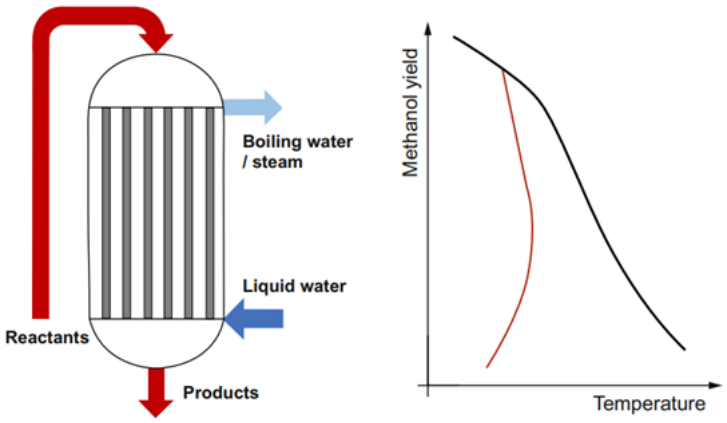

Figure 2.11: Isothermal boiling water reactor [6]

2.8 Research gap and objectives

This section identifies the research gaps found after the extensive literature review as follows:

- Lack of detailed data on the MSW composition needed as input in Aspen Plus. Often, only proximate or ultimate analysis is stated, or the composition is expressed in general terms such as plastics, organic fraction, etc.

- Although gasification kinetics are available for different biomass types like wood, this is not the case for MSW. Given the variability and complexity of the feedstock, there is lack of understanding about the gasification kinetics, resulting in a less rigorous model in Aspen Plus.

- Most of the literature on methanol synthesis kinetics focuses on the CO_2 hydrogenation, aimed at processes using captured CO_2 and green H_2. However, the syngas produced from MSW contains a high amount of CO, making the CO hydrogenation of outmost importance in the kinetics. While a few articles include both CO and CO_2 hydrogenation reactions in the conversion kinetics from syngas to methanol, they often use expensive catalysts that differ from common commercial ones.

- There is limited information about the formation of tar species and their kinetics. The majority of studies simplify the modeling process by omitting tar formation.

The objectives of this project with respect to the research gap are:

- To simulate the gasification of MSW as a fuel for methanol in Aspen Plus, including the formation of tar species and both CO and CO_2 hydrogenation reactions in the methanol synthesis reactor.

- To conduct a technoeconomic assesment of the process to evaluate its feasibility, using literature data when the model is not rigorous and Aspen does not provide accurate data, such as the gasifier.

3
Methods

3.1 Simulation setup

The complete conversion of MSW to methanol via gasification is simulated in Aspen Plus software, using the RK-Soave thermodynamic property model. This property method is suitable for gaseous mixtures, especially those containing H_2, CO, CO_2, H_2O, and CH_3OH, under high temperatures and pressures, making it a common choice for gasification-based models [55]. Additionally, the NRTL property method is selected for modeling the distillation section under low pressure. The binary interaction parameters for both models are available in the pure components databank of Aspen Plus [55] .

Additionally, the MIXCINC stream class is selected, comprising three sub-streams: MIXED, containing all vapor and liquid compounds, and Conventional Inert solid (CI) and Non-Conventional solid (NC), both containing solid compounds, with and without defined molecular weights, respectively [56]. The MSW feedstock is defined as a non-conventional compound, specifying its ultimate (ULTANAL) and proximate (PROXANAL) analyses, and its enthalpy and density are calculated using the HCOALGEN and DCOALIGT methods in Aspen [41]. The ash is also defined as a non-conventional compound, with 100% fixed ash content in both analyses [41]. Moreover, the char is assumed to be 100% carbon and is set as CI solid.

The process flowsheet for the model developed in Aspen Plus is shown in Figure 3.1. In this model, the MSW is dried before entering the BFB gasifier, where syngas is produced. After that, impurities in the syngas, including particulate solid matter, tar, and acid gases, are removed in a cleaning stage. Then, the H_2/CO ratio is adjusted to 2.5 in a conditioning step with a WGS reactor before the syngas enters the methanol synthesis reactor for conversion into methanol. After cooling down the products, part of the unconverted reactants is purged from the system while the rest is recycled back. Finally, the crude methanol is purified through a series of flash steps and a distillation column.

The following assumptions were made when modelling this process:

- The process is designed for a thermal input of 100 MW_{th} of MSW
- Steady-state and continuous operation
- Char is assumed to be 100% pure solid carbon
- Ash is inert
- Devolatilization in the pyrolysis stage is instantaneous
- No unconverted carbon
- Tar consists of phenol, toluene, and naphthalene

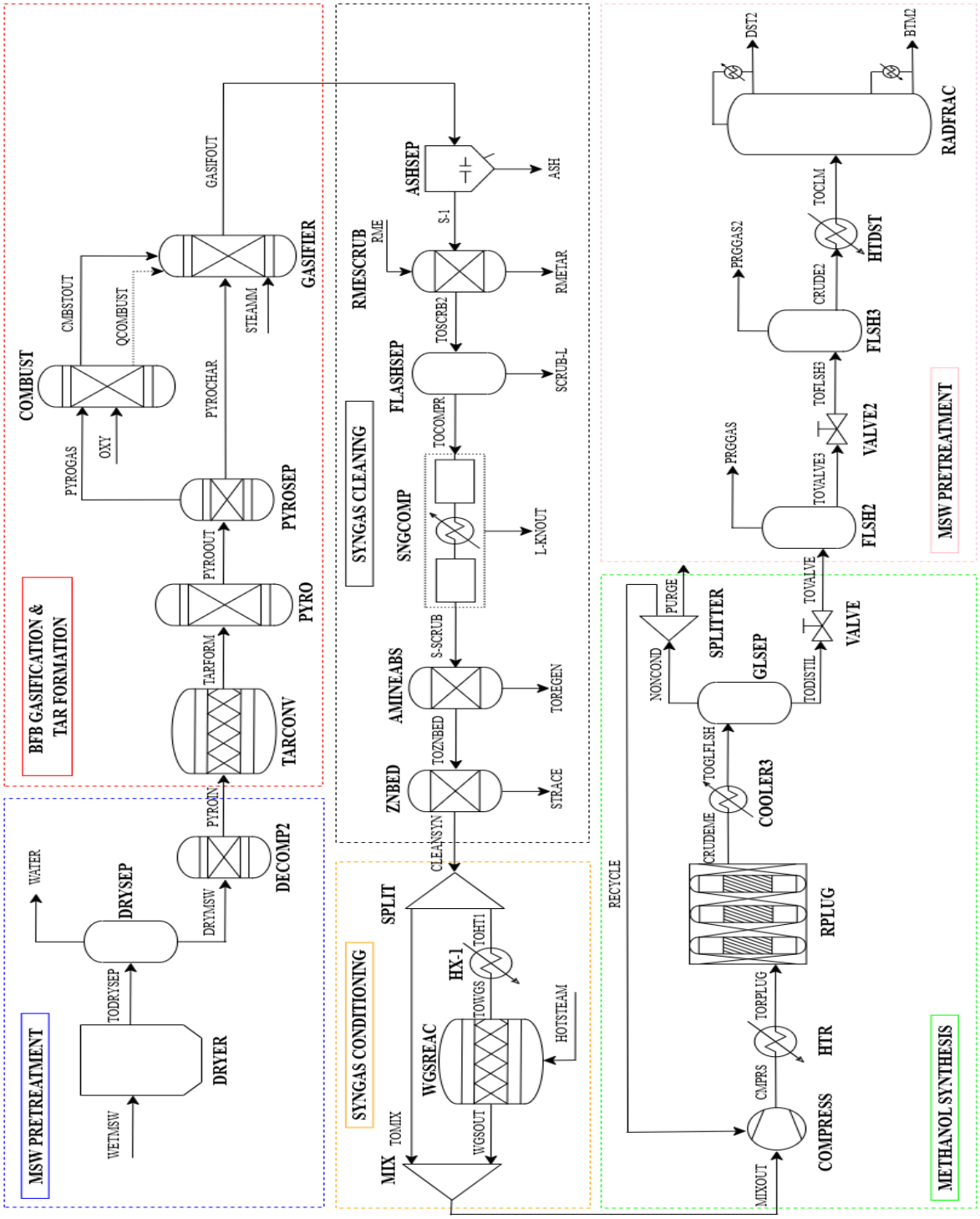

Figure 3.1: Process flow diagram

3.1.1 MSW composition

For this project, the Norwegian MSW reported in [8] is used. This selection is based on all the required input in Aspen being readily available, as well as the similarities with MSW from Sweden. Both the proximate and ultimate analyses are required as input in Aspen and are provided in Table 3.1 and Table 3.2 respectively. Additionally, sulfur analysis is required in Aspen (SULFANAL). Since it is not provided in the literature, it is assumed to follow the same distribution among the pyritic, sulfate, and organic fractions as coal, with their sum equal to the sulfur mass percentage reported in the ultimate analysis.

Table 3.1: Proximate analysis [8]

Component	Value
Moisture (%wb)	6.3
Volatile matter (%db)	78.6
Fixed carbon (%db)	9.0
Ash (%db)	12.4

Table 3.2: Ultimate analysis [8]

Component	Value (%db)
C	51.6
H	6.3
O	28.7
N	0.8
S	0.2
Ash	12.4

Since MSW is specified as a non-conventional component in Aspen, the heat of combustion (HCOMB), also referred to as Lower Heating Value (LHV), must be specified, and is calculated based on the CEN standard method [57] in Equation 3.1 below, where H, O, and N are the mass percentages of hydrogen, oxygen, and nitrogen reported in the ultimate analysis, respectively. Moreover, the High Heating Value (HHV) is considered as the average of the values reported in Table 3.3, calculated with different empirical formulas [57]. The MSW mass flow rate is calculated by dividing the process thermal input of 100 MW_{th} by the HHV as received.

$$\mathrm{LHV_{db}} = \mathrm{HHV_{db}} - 0.2122 \cdot H - 0.0008 \cdot (O + N) \tag{3.1}$$

Table 3.3: HHV values in dry basis [8]

Empirical formula	**HHV$_{db}$ (MJ/kg MSW)**
Boie	22.3
Dulong	21.3
Gaur& Reed	21.7

3.1.2 MSW pretreatment

Although the MSW composition for this project does not contain a significant amount of moisture, there is great variability in the composition seasonally and geographically. Therefore, a drying stage is modeled using an RStoic reactor (DRYER) and a Flash2 separator (DRYSEP), as shown in Figure 3.2. Since MSW is specified as a non-conventional component, Aspen assumes it has a molecular weight of 1 g/mol. Despite the drying stage not being considered a chemical reaction, the RStoic block is set up so that a portion of MSW transforms into water. More specifically, 1 mol of MSW reacts to form 0.0555084 moles of water [58].

The drying extent is controlled by a calculator block (WATER), as described in detail in Table B.1 in Appendix B. This calculator block overrides the fractional conversion of MSW according to the specified final moisture content in the dry MSW, set at 5%. Then, the DRYSEP block separates the water vapor formed from the dry feedstock.

Moreover, MSW must be converted into conventional type before entering the gasification stage, since the reactor units cannot process non-conventional components. Therefore, an RYield reactor (DECOMP2) is used to convert MSW into its conventional elemental constituents. The mass yields are initially specified and then overridden by a calculator block (DECOMP), as described in detail in Table B.2 in Appendix B, which calculates these yields based on the proximate and ultimate analysis through a mass balance. The description of the units involved in the MSW pretreatment is summarized in Table 3.4.

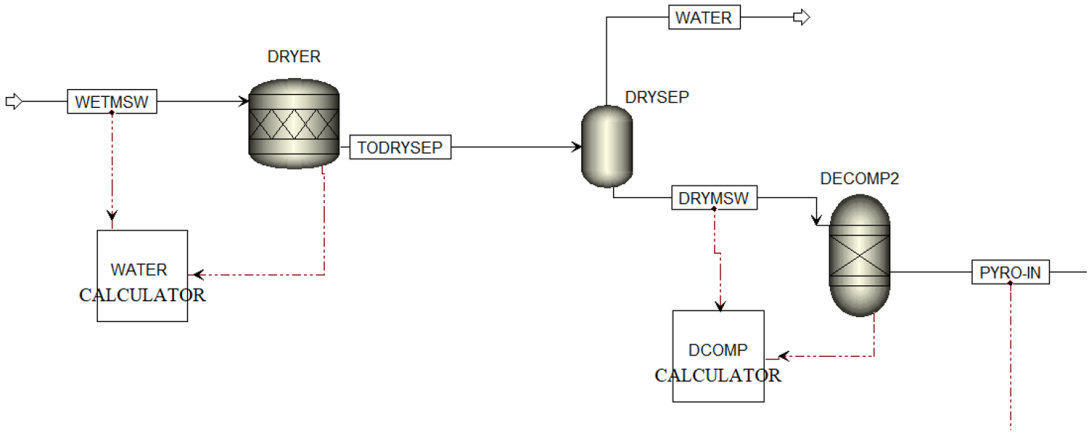

Figure 3.2: MSW drying and decomposition

Table 3.4: MSW pretreatment units

Block	Description
DRYER (RStoic)	Simulates the feedstock drying stage according to: MSW $\rightarrow$ 0.0555084 H_2O Fractional conversion of MSW is initially specified and the value is overridden by the calculator block WATER detailed in Table B.1 in Appendix B.
DRYSEP (Flash2)	Separates the water vapor formed in DRYER from the dry MSW
DECOMP (RYield)	Transforms non-conventional MSW into its conventional constituents by calculating their mass yields through a mass balance based on the proximate and ultimate analysis by the calculator block DECOMP, detailed in Table B.2 in Appendix B

3.1.3 BFB gasification and tar formation

Given the complexity and significant variability in the composition of MSW, the kinetics of its gasification process are still under study. Therefore, rather than using a kinetic reactor or a gasifier block in Aspen for modeling, the process (Figure 3.3) is divided into four main stages:

- Tar formation
- Devolatilization
- Volatiles combustion
- Char gasification

Although these processes are modeled as four separate stages, in reality, they occur simultaneously within the bubbling fluidized bed (BFB) gasifier.

After the dried MSW is decomposed into its elemental major constituents, it enters an RStoic block (TARCONV), where the formation of tar, assumed to consist of phenol, toluene, and naphthalene, is simulated. The model for tar formation is adopted from Roshan et al. (2022) [27] and Shahrivar et al. (2022) [56], using a Calculator Block (TARCONV) detailed in Table B.3 of Appendix B. This block calculates the fractional conversion of carbon into the different tar species as a function of the gasifier operating temperature and the specified total amount of tar formed. After the formation of phenol, toluene, and naphthalene, these species are specified as inert in the subsequent blocks.

Then, the pyrolysis stage, in which the volatile compounds are released from the feedstock, leaving char and ash behind, is simulated in an RGibbs block (PYRO) at 500 °C. This phase and chemical equilibrium reactor operates based on the minimization of Gibbs free energy. After that, the volatile compounds are virtually separated from the char and ash solid fractions in a Sep block (PYROSEP).

The volatiles are combusted in another RGibbs block (COMBUST) with oxygen (OXY) to supply the necessary heat to support the endothermic gasification reactions. The mass flow of oxygen injected in this block is adjusted with a design specification (AUTOTHER), as described in Table C.1 of Appendix C, to ensure the heat duty of the gasifier block (GASIFIER) is zero, achiveving autothermal operation. While not explicitly modeled, the oxygen stream is sourced from an air separation unit, which will be accounted for in the plant costs.

Analogous to the volatile combustion stage, char gasification with steam is modeled using another phase and chemical equilibrium RGibbs reactor (GASIFIER) at 920 °C, where carbon conversion is assumed to be 100%. In this block, the equilibrium

results in the nitrogen in the MSW being primarily converted to NH_3 and N_2, while sulfur is almost entirely converted to H_2S. Additionally, the steam mass flow injected in the gasifier at 235 °C and 1 atm is adjusted with a design specification, described in Table C.2 in Appendix C, to maintain a steam-to-feedstock ratio (S/F) of 0.8, which was set based on a sensitivity analysis. If the S/F ratio is too low, the syngas will be deficient in hydrogen since steam acts as a hydrogen source. Conversely, if the S/F ratio is too high, the steam reforming reaction rate is reduced due to the cooling effect of excessive steam, which also increases energy requirements. After that, the syngas will be cooled down and will undergo a thorough cleaning stage. The description of the units involved in the MSW gasification is summarized in Table 3.5.

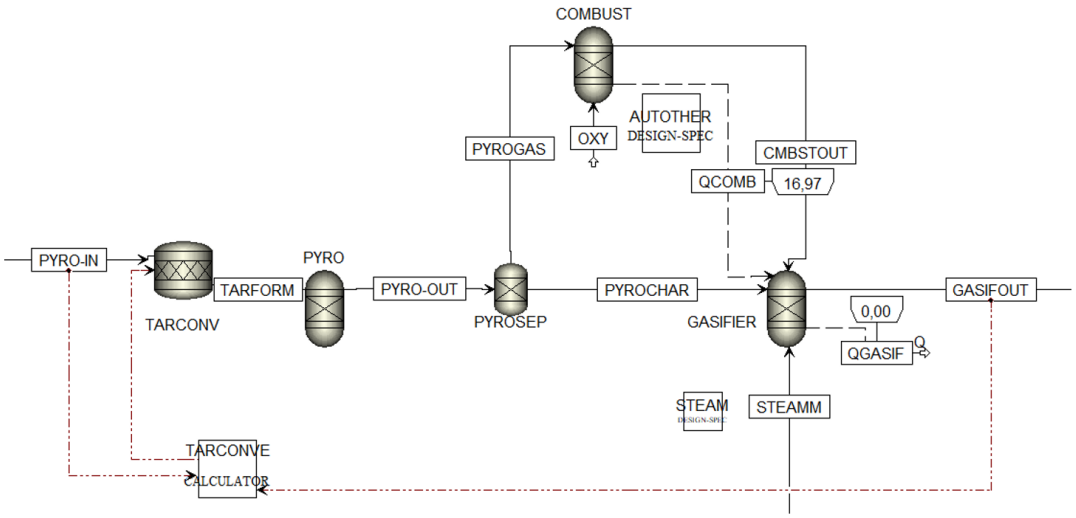

Figure 3.3: MSW gasification and tar formation

Table 3.5: MSW gasification and tar conversion description

Block	Description
TARCONV (RStoic)	This block models the formation of tar, assumed as only phenol, toluene, and naphthalene, according to the reactions: $6\,C + 3\,H_2 + 0.5\,O_2 \longrightarrow C_6H_5OH$ (phenol) $7\,C + 4\,H_2 \longrightarrow C_6H_5CH_3$ (toluene) $10\,C + 4\,H_2 \longrightarrow C_{10}H_8$ (naphthalene) The amount formed of each tar species is controlled by a calculator block (TARCONVE) based on literature data and adopted from [56].
PYRO (RGibbs)	Models the instantaneous devolatilization stage as a phase and chemical equilibrium at 500°C and 1 atm. The selected possible mixed products are: H_2O, O_2, CO, CO_2, S, SO_2, H_2S, N_2, and NH_3. C was selected as Pure Solid and toluene, phenol, and naphthalene as inert species.
PYROSEP (Sep)	Separates the gaseous volatile compounds from the solid ash and char fractions after the pyrolysis stage.
COMBUST (RGibbs)	Models the combustion of volatiles with oxygen. The mass flow of oxygen is controlled using a design specification (Table C.1 in Appendix C) to ensure that the heat released from the combustion reactions precisely matches the requirements of the gasifier, resulting in a heat duty of zero. The selected possible mixed products are: H_2O, O_2, CO, CO_2, S, SO_2, H_2S, N_2, and NH_3. Toluene, phenol, and naphthalene as inert species.
GASIFIER (RGibbs)	Models the steam-char gasification reactions at 920°C and 1 atm in autothermal operation. The selected possible mixed products are: H_2O, O_2, CO, CO_2, S, SO_2, H_2S, N_2, and NH_3. Toluene, phenol, and naphthalene as inert species, and char has a 100% conversion. Design spec in Table C.2 of Appendix C is used to adjust the S/F ratio to 0.8 by calculating the steam mass flow at 235°C and 1 atm.

3.1.4 Syngas cleaning

To remove the syngas impurities after gasification, including ash, tars, hydrogen sulfide, ammonia, and water, several cleaning steps are required. These stages, shown in Figure 3.4, are modeled following the detailed model described by Arvidsson et al. (2014) [59], ignoring the pressure drops in the units.

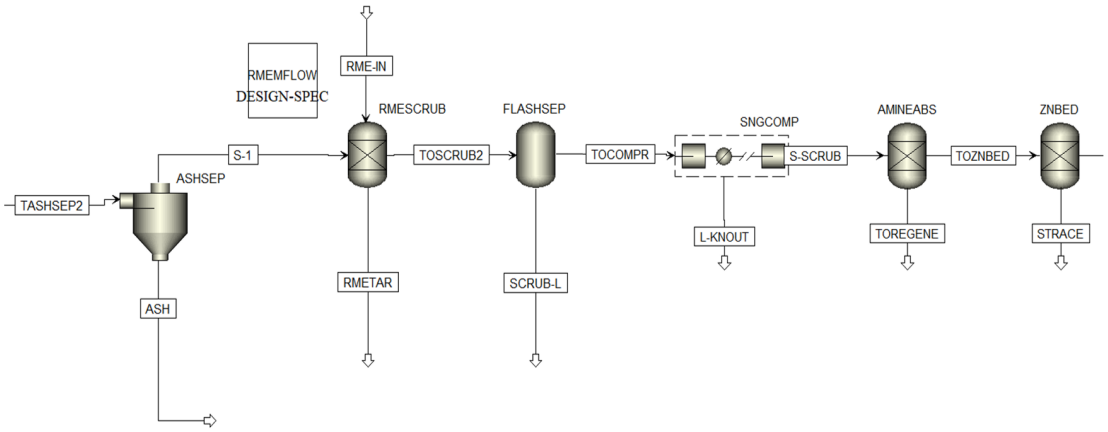

Figure 3.4: Syngas cleaning

The syngas leaving the gasifier at 920 °C must be cooled down to 110 °C before entering the fabric filter (ASHSEP) since its performance is hindered by high temperatures. This SSplit block simulates the removal of particulate matter, all assumed as fly ash, with 100% removal efficiency. After that, the ash-free syngas enters the Rapeseed Methyl Ester (RME) scrubber for tar removal, modeled as a Sep block (RMESCRUB) and a Flash2 block (FLASHSEP). The RME absorbs all the tar in the syngas, and its mass flow consumption, controlled by the design specification (RMEFLOW) described in Table C.3 of Appendix C, is assumed to be 2.4% of the energy rate on an HHV basis of the syngas exiting the tar scrubber [59]. In the FLASHSEP block, some water and ammonia are removed. After that, the syngas is compressed to 30 bar in a 3-stage compressor with intercooling and knockout drums, further removing water before the acid gas removal stage.

Then, the syngas at 40 °C passes through a conventional amine absorber and a Zinc oxide guard bed, both modeled as Sep blocks (AMINEABS, ZNBED), for removing acid gases and trace impurities. The amine absorber (AMINEABS) is assumed to use Methyl Diethanolamine (MDEA) as solvent with molar absorption efficiencies of 96%, 62%, 100%, 0.0738%, and 0.0581% for H_2S, CO_2, NH_3, CH_4, and CO, respectively [56]. Lastly, the remaining H_2S traces are removed in the

Zinc oxide guard bed to avoid catalyst poisoning in the posterior stages. The description of the units involved in the syngas cleaning is summarized in Table 3.6.

Table 3.6: Syngas cleaning units

Block	Description
ASHSEP (RStoic)	Fabric filter that removes fly ash from the syngas with 100% efficiency.
RMESCRUB (Sep)	Ash-free syngas is mixed with RME at 25 °C. This block models the tar absorption in the RME as a component separator. The mass inflow of RME is controlled by the design spec described in Table C.3 of Appendix C.
FLASHSEP (Flash2)	Simulates the water removal of the RME scrubber.
SNGCOMP (MCompr)	Simulates a 3-stage isentropic compressor with equal pressure ratios, intercooling stages, and knockout drums between compression stages to remove liquid components (mainly water) from the syngas. The outlet temperature of the first two intercooling stages is 80 °C, and the syngas is released at 40 °C in the final cooler.
AMINEABS (Sep)	Amine scrubber modeled as a component separator with split molar fractions of 96%, 62%, 100%, 0.0738%, and 0.0581% for H_2, CO_2, NH_3, CH_4, and CO, respectively.
ZNBED (Sep)	Simulates a Zinc oxide guard bed that removes 100% H_2S.

3.1.5 Syngas conditioning

The clean syngas enters a conditioning stage, shown in Figure 3.5, before the methanol synthesis to adjust its H_2/CO ratio to the ideal value for chemical synthesis of 2.5 [41][49]. The WGS adiabatic reactor is modeled as an RStoic block (WGSREAC) operating at 350 °C and 30 bar [59] [69], specifying the stoichiometric water gas shift reaction with a CO conversion efficiency of 70% [60][70]. The syngas stream is split into two: one part bypasses the reactor, while the other is preheated to 350 °before entering the reactor. The split fraction of the syngas entering the reactor is controlled by the design specification described in Table C.4 of Appendix C, achieving the target H_2/CO ratio.

Additionally, steam (HOTSTEAM) is injected into the reactor at 350 °C and 30 bar for the reaction to occur. The mass flow of superheated steam is regulated by the design specification described in Table C.5 of Appendix C, ensuring that the H_2O/CO within the reactor is 1.5 to reduce the risk of carbon deposition[56], [61]. Finally, the product stream exiting the reactor is mixed in the MIX block with the bypassed syngas, resulting in a syngas with the targeted H_2/ CO ratio of 2.5. The description of the units involved in the syngas conditioning is summarized in Table 3.7.

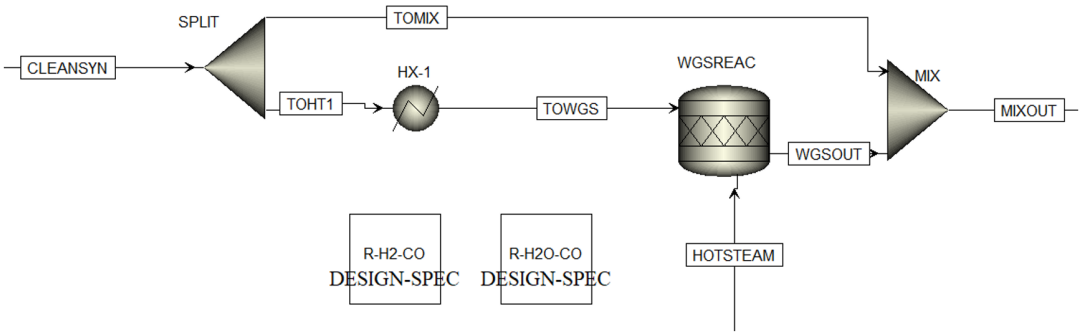

Figure 3.5: Syngas conditioning

Table 3.7: Syngas conditioning units

Block	Description
SPLIT (FSplit)	Splits the clean syngas into two. The split fraction of the stream entering the reactor is controlled by the design specification in Table C.4 in Appendix C so that the H_2/ CO ratio after the WGS reactor is 2.5.
HX1	Heats up the syngas entering the reactor up to 350 °C. Heat exchanger with the syngas exiting the gasifier. See Section 3.1.8
WGSREAC (RStoic)	Simulates an adiabatic WGS reactor at 350 °C and 30 bar, with steam injection at the same conditions and a CO conversion of 0.7 (WGS reaction). The steam mass flow is adjusted with the design specification in Table C.5 in Appendix C, so that the H_2O/ CO ratio within the reactor prevents carbon deposition.
MIX (Mixer)	Mixes the syngas exiting the WGS reactor and the bypassed syngas.

3.1.6 Methanol synthesis

After the conditioning stage, methanol is synthesized from syngas in the reaction-reparation-recycling system described in Figure 3.6 [55]. The syngas is compressed to 70 bar in an isentropic compressor (COMPRESS) and heated up to 220 °C before entering the vapor phase synthesis reactor, modeled as an RPlug block (RPLUG). The kinetic model (LHHW) implemented in the reactor is adopted from Kiss et al. (2016) [55], and includes both CO and CO_2 hydrogenation as well as the reverse WGS reaction, using an excess of Cu/Zn/Al/Zr fibrous catalyst. All the equations for methanol synthesis are described in Equations 2.7, 2.8, and 2.9, respectively, in Section 2.7. While the length and diameter are kept the same as in the original study, the number of tubes in this multitubular reactor was modified to achieve a similar residence time of approximately 14 seconds, given the different volumetric flows.

The gaseous mixture exiting the reactor contains both products, like methanol, and unconverted reactants, like CO and H_2. These gases are cooled down and flashed in a Flash2 block (GLSEP), where the non-condensable gases are separated from the liquid crude methanol. After a 5 % purge (SPLITTER) to avoid deposition in the reactor, the non-condensable fraction is recycled back and mixed with the fresh clean syngas before compression. The description of the units involved in the methanol synthesis is summarized in Table 3.8.

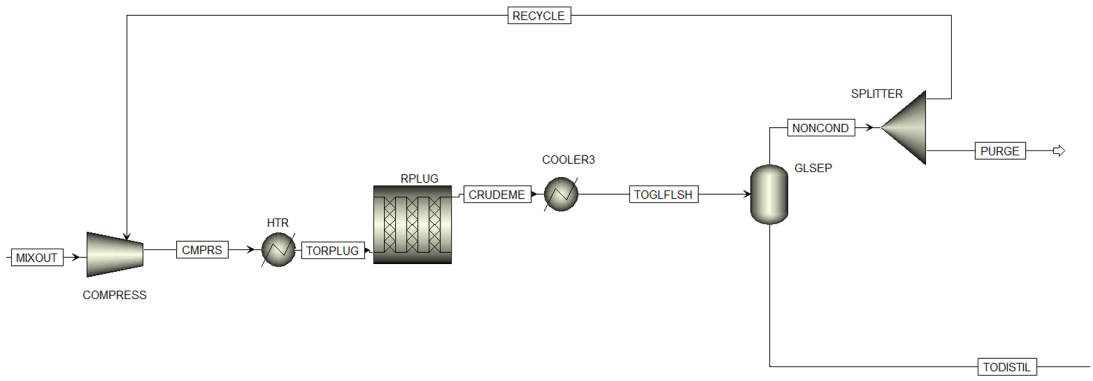

Figure 3.6: Methanol synthesis

Table 3.8: Methanol synthesis units

Block	Description
COMPRESS (Compress)	Simulates an isentropic compressor with an oultet pressure of 70 bar. Both the fresh clean syngas and the recycled non-condensable reactants are compressed in this unit.
HTR, COOLER3 (Heater)	Heat up to 220 °C before the reactor, cool down to 30 °C after the reactor. Heat integration with heat exchanger. See Section 3.1.8
RPLUG (RPlug)	Simulates a medium pressure methanol synthesis reactor using the kinetic model (LHHW) from Kiss et al. (2016) [55].The pressure drop is calculated using the Ergun frictional correlation. The operating conditions are 220 °C and 70 bar with a Cu/Zn/Al/Zr catalyst loading of 865 kg and a bed voidage of 0.98. The residence time of the gases is 13.8119 sec, with reactor dimensions of L=12 m, ϕ= 0,06 m, and 534 tubes.
GLSEP (Flash2)	This block flashes the product gas mixture at 30 °C and 40 bar, resulting in a liquid crude methanol stream that goes to the subsequent purification step, and gaseous stream with unconverted reactants that will be recycled to the reactor.
SPLITTER (FSPlit)	his block purges 5% of the non-condensable reactants before they are recycled back to avoid their accumulation and deposition in the reactor.

3.1.7 Methanol purification

The model for methanol purification using a distillation process is adopted from Van-Dal et al. (2013) [62]. The liquid stream that separated from the unconverted gaseous reactants contains methanol, water, and residual dissolved gases. This crude methanol is expanded to 10 bar and then to 1.2 bar in two separate valves (VALVE, VALVE2) with intermediate flash tanks (FLSH2, FLSH3) to remove the residual gases, as shown in Figure 3.7.

The resulting stream is heated up to 54 °C before entering the equilibrium-based distillation block (RADFRAC). Prior to the RADFRAC simulation, a DSTWU block was used to estimate the number of equilibrium stages and the reflux ratio, serving as the starting point for the RADFRAC block. After 25 equilibrium stages, with the feed introduced at the 19th stage, the distillate, containing methanol with a molar purity of 99.3%, exits the column at approximately 40 °C, while the bottom fraction consisting of water leaves at 93.9 °C. The description of the units involved in the methanol synthesis is summarized in Table 3.9.

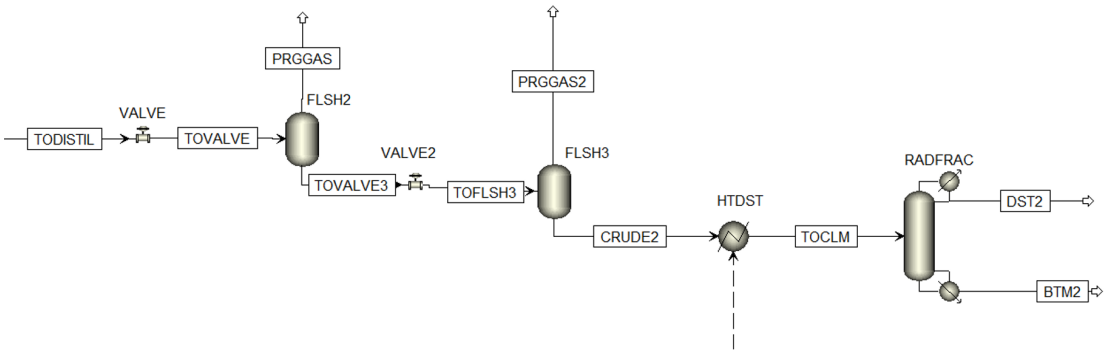

Figure 3.7: Methanol purification

Table 3.9: Methanol purification units

Block	Description
VALVE, VALVE2 (Valve)	Expands the crude methanol to 10 bar and to 1.2 bar respectively.
FLSH2, FLSH3 (Flash2)	Flash blocks that separate the dissolved gases, mainly CO_2 , from the liquid fraction.
HTSDT (Heater)	Heats up the feed stream up to 54 °C. Heat integration with heat exchanger. See Section 3.1.8
RADFRAC (Radfrac)	Equilibrium-based distillation column with 25 equilibrium stages, feed at the 19^{th} stage entering at 54 °C, and a total condenser.The molar reflux ratio is 1.8, and the distillate rate is 9500 kg/h, based on sensitivity analyses aimed at achieving the highest possible methanol molar purity, which reaches 99.3%.

3.1.8 Heat integration

Once the model was setup, an analysis of heat and cooling demands was performed manually to enable heat integration. There are two major divisions, steam generation at high and low pressures to supply the WGS reactor and the gasifier, respectively, and the heating up of the syngas before the methanol reactor.

In Figure 3.8, a schematic representation of the steam generation within the process is shown. In the first heat exchanger, steam at 350 °C and 30 bar is generated by cooling down the hot syngas to 534.31 °C. Then, the syngas is cooled further while preheating the stream entering the WGS reactor at 350 °C. Finally, the low pressure steam needed in the gasifier is generated by cooling the syngas to 110 °C. This low pressure steam is superheated to 235 °C by exchanging heat with the third intercooling stage in the syngas compressor from the syngas cleaning stage. Note that all the required water and steam mass flows are previously determined

by design specifications.

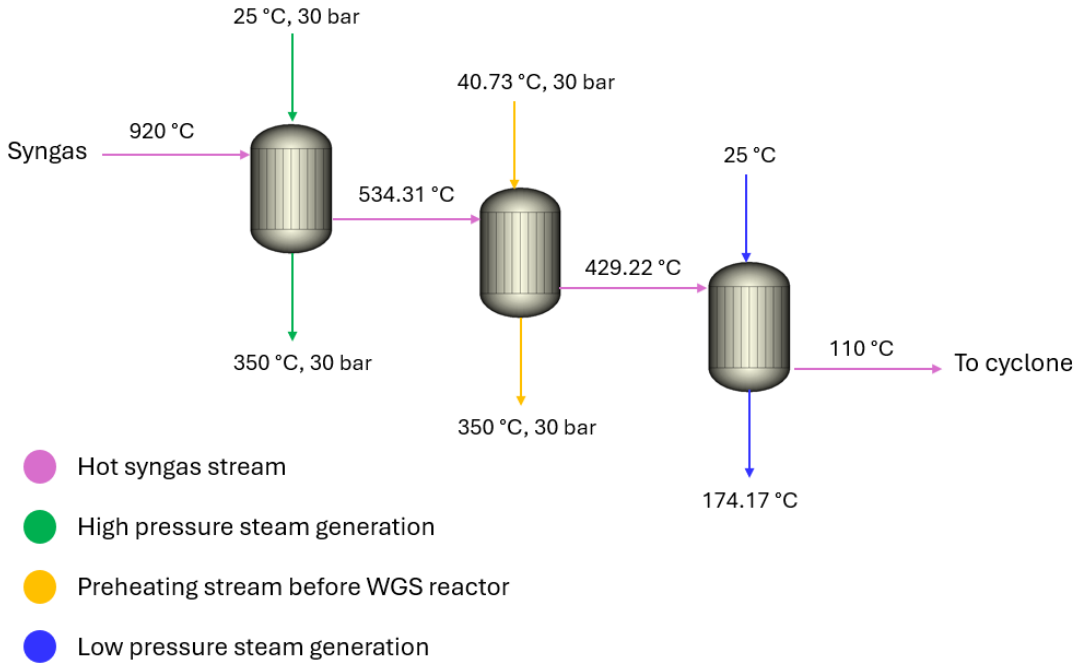

Figure 3.8: Steam generation

Moreover, Figure 3.9 shows a schematic diagram for the heat integration in the methanol loop. First, the syngas is heated up to 210 °C by the outlet stream from the reactor at 220 °C, keeping a feasible ΔT_{min} (5 °C) . The rest of the heat is supplied by the second intercooling stage from the syngas compressor in the syngas cleaning step, represented by the blue dotted arrow in the figure. On the other hand, the outlet gas mixture from the reactor is further cooled down by preheating the stream entering the distillation column. Laslty, the rest of the cooling requirement is supplied by cooling water, reaching 31 °C before the flash and separation step.

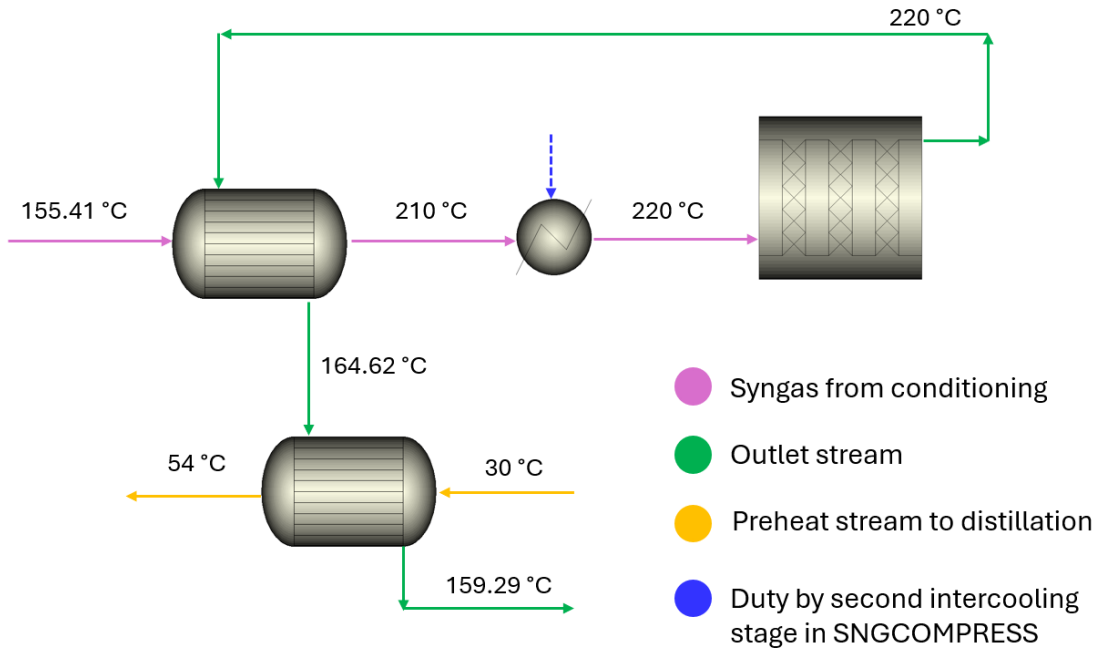

Figure 3.9: Heat in the methanol loop

3.2 Efficiency parameters

This section aims to outline several key process parameters that provide insights into process performance and identify potential areas for improvement.

3.2.1 Overall process energy efficiency

The overall energy efficiency, or thermal efficiency based on the lower heating value (LHV), of the process, is determined by the ratio of the useful energy output to the required energy input, shown in Equation 3.2 [63]. The useful energy output encompasses the methanol produced minus the net electricity consumption, whereas the required energy input refers to the MSW fed to the plant.

$$\eta = \frac{\text{Energy output}}{\text{Energy input}} = \frac{\dot{m}_{\text{MeOH}} \cdot \text{LHV}_{\text{MeOH}} \pm W_{\text{el,net}}}{\dot{m}_{\text{MSW}} \cdot \text{LHV}_{\text{MSW}}} \tag{3.2}$$

3.2.2 Cold Gas Efficiency (CGE)

The cold gas efficiency measures how much chemical energy is in the clean syngas produced during gasification over the total energy in the feedstock and is calculated

following Equation 3.3 below [64]. To convert the LHV from a dry basis to a wet basis, Equation 3.4 [57] is used.

$$\mathrm{CGE} = \frac{\dot{m}_{\mathrm{syng,cl}} \cdot \mathrm{LHV}_{\mathrm{syng,cl}}}{\dot{m}_{\mathrm{MSW,wb}} \cdot \mathrm{LHV}_{\mathrm{MSW,wb}}} \tag{3.3}$$

$$\mathrm{LHV}_{\mathrm{wb}} = \mathrm{LHV}_{\mathrm{db}} \cdot (1 - \mathrm{MC} \cdot 0.01) - 2{,}433 \cdot \mathrm{MC} \cdot 0.01 \tag{3.4}$$

3.2.3 Carbon efficiency

The carbon efficiency is an important metric that evaluates the conversion effectiveness of the feedstock into methanol. This efficiency is calculated as the ratio of carbon atoms in the methanol product to the total carbon atoms in the MSW, as shown in Equation 3.5. The greater the value, the more effective utilization of the feedstock, which is advantageous both economically and environmentally [65].

$$\eta_c = \frac{\text{C in product}}{\text{C in feedstock}} = \frac{\dot{m}_{\mathrm{MeOH}} \cdot X_{C,\mathrm{MeOH}}}{\dot{m}_{\mathrm{MSW}} \cdot X_{C,\mathrm{MSW}}} \tag{3.5}$$

3.3 Economic analysis

This section outlines the methodology to carry out the economic analysis to assess the preliminary feasibility of the project.

3.3.1 Capital cost

The capital cost of the process, also referred to as capital expenditure (CAPEX), represents the expenses necessary for the setup and startup of the plant, including costs for equipment purchasing, installation, facilities, infrastructure, materials, engineering fees, labor, land acquisition, and contingency funds [9] . The CAPEX can be divided into fixed capital, calculated based on equipment purchase cost, and working capital, usually estimated as 15% of the fixed capital [9]. The working capital, needed for the startup of the plant, may be recovered when the plant reaches the end of its operational lifetime. Therefore, total capital cost of this project will be the sum of the fixed and working capitals.

The delivered equipment cost, which is a function of size, material, and operating conditions, is often calculated based on Equation 3.6, a power law expression that relates cost to capacity, in which C_E is the equipment cost with size S_E, C_B is the known base cost for equipment with size S_B, and M is a scale factor that depends

on the equipment type [9]. The data for C_B, S_B, and M is based on literature (reported in Table 3.11).

$$C_E = C_B \cdot \left(\frac{S_E}{S_B}\right)^M \tag{3.6}$$

The autothermal bubbling fluidized bed cost is calculated as detailed in Swanson et al.(2010) [66] and is evaluated at 300 short tons per day (tpd), the maximum proven capacity for this gasifier type. Therefore, multiple fluidized-bed gasifiers with the upper limit capacity are used in parallel, assuming that the train formula outlined in Equation 3.7 is followed, where N is the number of trains, and m is an exponent with a typical value of 0.9.

$$C_{\text{train}} = C_E \cdot N^m \tag{3.7}$$

Due to inflation, new technology developments, and market fluctuations, the cost of equipment changes over time, so the cost data must be updated. This is achieved using the Chemical Engineering Plant Cost Index (CEPCI), as shown in Equation 3.8, where the subindex 0 denotes the reference year and the subindex i represents the year to which it is being updated.

$$C_{E,i} = C_{E,0} \cdot \left(\frac{\text{CEPCI}_i}{\text{CEPCI}_0}\right) \tag{3.8}$$

After the delivered equipment costs are updated, the total cost of the physical plant is estimated by multiplying the total equipment costs by an average factor that accounts for both direct and indirect installation costs, as shown in Equation 18 [9].

$$\text{Fixed Capital} = f_I \cdot \sum_i C_{E,i} \tag{3.9}$$

The overall installation factor for the complete system f_I is the sum of the components detailed in Table 3.10 [9], categorized based on the dominant phase being processed, whether solid or fluid. For this process, which involves a mixture of solid and fluid stages, the contributions to the capital cost can be calculated by interpolating between the two extreme values, based on the ratio of major processing steps classified as either fluid or solid processing [9].

The delivered equipment cost data from literature is detailed in Table 3.11, and the cost data for the heat exchanger network is taken from Aspen Plus. Since the literature data is in U.S dollar, the average conversion rate for 2024 to euros (1 USD= 0.9240 EUR) is used [67].

Table 3.10: Typical direct and indirect cost factors based on delivered equipment cost [9]

Item	Process Type	
	Fluids	**Solids**
Major equipment, total purchase cost	$C_{E,i}$	$C_{E,i}$
Equipment erection, f_{ER}	0.4	0.5
Piping, f_{PIP}	0.7	0.2
Instrumentation and control, f_{INST}	0.2	0.1
Electrical, f_{ELEC}	0.1	0.1
Utilities, f_{UTIL}	0.5	0.2
Off-sites, f_{OS}	0.2	0.2
Building (including services), f_{BUILD}	0.2	0.3
Site preparation, f_{SP}	0.1	0.1
Indirect costs		
Design, engineering, and construction, f_{DEC}	1	0.8
Contingency (about 10% of fixed capital cost), f_{CONT}	0.4	0.3

Table 3.11: Delivered equipment costs based on literature data

Equipment	**Size units**	**Size**	**T [°C]**	**P**	**Base size**	**Base cost (M$)**	**Scale factor M**	**Ref. year**	**CEPCI (ref. year) [68]**	**Refs**
MSW handling/feeding	Wet tonne/h	16.54	25	1 atm	33.5	0.48	1	2002	395.6	[69]
Drier	kg H_2O evap/h	226.30	110	1 atm	700	0.23	0.65	2000	394.1	[9]
BFB autothermal gasifier	Syngas tonne/h	16.31	920	1 atm	41.7	6.41	0.7	2003	402	[66]
Fabric filter	Syngas m^3/s	17.82	110	1 atm	15.6	0.068	0.6	2002	395.6	[70]
RME scrubber	Syngas m^3/s	13.05	110	1 atm	14.7	1.64	0.7	2002	395.6	[69]
SNG compressor	Power (kW)	4258.10	40	30 bar	250	0.0984	0.46	2000	394.1	[9]
Amine absorber	Syngas m^3/s	0.302	40	30 bar	12.1	3	0.7	2002	395.6	[69]
ZnO guard bed	Syngas m^3/s	0.274	40	30 bar	8	0.024481	1	2002	395.6	[69]
WGS reactor	CO+H_2 kmol/h	522.4	350	30 bar	8819	12.2	1	2002	395.6	[69]
Compressor to reactor	Power (kW)	5502.14	-	70 bar	250	0.0984	0.46	2000	394.1	[9]
Methanol reactor	Tonne MeOH/h	10.76	220	70 bar	87.5	7	0.6	2001	394.3	[71]
Distillation	Ton MeOH/yr	91797.2	-	1 bar	10000	1.36	0.7	2022	802.9	[72]
ASU	kg O_2/s	2.12	200	1 atm	32.45	45.5	0.67	2011	585.7	[63]
HX network - From Aspen Plus										

3.3.2 Operational cost

The operating cost of the process, also referred to as operating expenditure (OPEX), represents the expenses required to maintain and run the plant. It is commonly divided into fixed operating costs, and variable operating costs.

Fixed operating costs are independent of the production size and encompass the different categories detailed in Table 3.12 [73] .

Table 3.12: Fixed operating cost

Type	Value
Labor	0.5% of total capital cost [74]
Management & supervision	20% of labor cost
Maintenance	5% of fixed capital cost
Taxes	2% of fixed capital cost
Insurance	1% of fixed capital cost
R&D overheads	20% of variable operating costs

On the other hand, variable operating costs vary with production volume and typically include raw materials, catalyst loads, and energy consumption, as described in Table 3.13.However, in this case, MSW is not a cost but a revenue, since municipalities pay the companies to handle it. It is assumed that the catalyst has a lifespan of 5 years before requiring regeneration. Cooling water is needed for the cooling demands in the process, and electricity for the different equipment like pumps, compressors, and the ASU unit, which has a specific power consumption of 0.28 kW/Nm^3 [75]. These demands are taken directly from Aspen Plus.

Table 3.13: Variable operating cost

Type	Value
Catalyst & chemicals	1% of total fixed cost [74]
Cooling water	0.0449 €/cum [76]
Electricity	0.0493 €/KWh [77]

3.3.3 Economic parameters

This section outlines the different assumptions, detailed in Table 3.14 [78], and financial metrics used to assess the preliminary economic feasibility of the plant.

Table 3.14: Economic parameters

Parameter	Value
Plant location	Europe
Plant economic lifetime (yrs)	20
Base year	2024
CEPCI [68]	795.4
Plant operation mode	Continuous
Annual operating hours (h/yr)	8000
Interest rate (%)	10
Discount rate (%)	10
USD to EUR conversion (€/$)	0.924
SEK to EUR conversion (€/SEK)	0.08761
Methanol productivity (tonne/h)	9.5
Selling price of methanol (€/tonne) [79]	584.89

The cash flow approach, based on assessing the annual costs and revenues during the plant lifetime, is adopted for the economic analysis. The plant's revenue is generated from methanol production and a gate fee for municipal solid waste (MSW), assumed to be 65 €/tonne [80].
The following economic metrics are calculated to determine the preliminary economic viability of the plant:

Simple Payback Period (PBP)

The PBP is a simple economic parameter used to calculate the time needed to recover the initial investment, as described in Equation 3.10 [81]. However, it does not account for either the time value of money or the revenue after the investment is recovered.

$$\text{PBP} = \frac{\text{Total investment}}{\text{Average annual cash flow}} = \frac{I_0}{\left(\frac{\sum_{i=0}^{n} F_i}{n}\right)} \tag{3.10}$$

Where I_0 , F_i, and n are the initial investment, the cash flow in the year i, and the plant lifetime, respectively.

Return on Investment (ROI)

The ROI is a metric of how profitable an investment is by comparing the cumulative net profit to the initial investment, as shown in Equation 3.11 [81]. Like the PBP, the ROI does not account for the time value of money.

$$\text{ROI} = \frac{\text{Cumulative net profit}}{\text{Plant life} \cdot \text{Initial investment}} = \frac{\sum_{i=0}^{n} F_i}{n \cdot I_0} \tag{3.11}$$

Net Present Value (NPV)

The NPV of a project is the sum of the present values of the future cash flows, as described in Equation 3.12, where r is the discount rate, which considers the time value of money and the annual variation in costs and revenues [81].

$$\text{NPV} = \sum_{i=0}^{n} \frac{F_i}{(1+r)^i} \tag{3.12}$$

Levelized Cost of Methanol (LCoM)

Another relevant economic parameter is the Levelized Cost of Methanol (LCOM), which represents the minimum selling price of methanol required to achieve a net present value (NPV) of zero, or in other words, to reach the break-even point (neither profit nor loss) by the end of the plant's lifetime [82], and it can be calculated according to Equation 3.13.

$$\text{LCoM}\left(\frac{€}{\text{tonne}}\right) = \frac{\text{ACC} + \text{OPEX}}{\text{Annual MeOH production}} \tag{3.13}$$

Where ACC is the Annualized Capital Cost, calculated by multiplying the total investment cost by the Capital Recovery Factor (CRF), as expressed in Equation 3.14 below.

$$\text{ACC} = \text{Total Capital Cost (TCP)} \cdot \text{CRF} = \text{TCP} \cdot \frac{r \cdot (1+r)^n}{(1+r)^n - 1} \tag{3.14}$$

4

Results & Discussion

4.1 Model validation

The MSW fluidized bed gasification part of the model was validated using the experimental data from Hejazi et al. (2017) [10] and the validation results from the model by Puig-Gamero et al. (2018) [41], who used the same experimental data to validate their model. First, the composition used in the studies, detailed in Table 4.1 [10], was specified in Aspen. Additionally, the heat of combustion was adjusted according to that composition, and the model was simulated in the same conditions described in the studies, under 831 °C and 1 atm. The results for the syngas composition in vol % dry basis are compiled in Table 4.2, compared to the experimental results obtained by Hejazi et al. (2017) [10] and to the predicted composition in the model by Puig-Gamero et al. (2018) [41].

Table 4.1: Proximate and ultimate analysis of biomass used in Hejazi et al. (2017) [10]

Ultimate analysis (wt %)					**Proximate analysis (wt %)*daf**			
C	**H**	**N**	**S**	**O**	**Ash**	**VM**	**FC**	**Moist.**
50.8	6.26	0.22	0.10	41.6	1	81.7	17.3	5.4

Table 4.2: Syngas composition (vol.% dry basis) obtained with the simulation model and comparison to experimental data.

Compound	**Experimental composition in [10]**	**Predicted composition by [41]**	**My predicted composition**
H_2	45-55	57	59.5
CO	21-25	20	22.76
CO_2	18-22	18	16.4
CH_4	2-4	2.2	1.31

When comparing the different syngas compositions in Table 4.2, it is observed that

the H_2 vol% is overestimated in this model compared to the experimental values, whereas the CH_4 vol% is underestimated. The difference for H_2 is also perceived in the model by Puig-Gamero et al. (2018) [41], although to a lesser extent. This discrepancy arises from the RGibbs block, based on a phase and chemical equilibrium model, which predicts almost complete CH4 conversion, thereby increasing hydrogen production [83]. However, real gasifiers have a short residence time so thermodynamic equilibrium is not reached, leading to lower CH_4 and higher H_2 values in simulations using equilibrium modeling [83]. Additionally, char has been assumed to be 100% carbon, but in reality, char contains other components that potentially release CH_4, contributing to the underestimation.

4.2 Process parameters

For a MSW input of 100 MW_{th}, with a $LHV_{MSW,\,db}$ of 20.41 MJ/kg, the main process parameters are reported in Table 4.3 below. These values were obtained for a gasifier temperature of 920 °C and a methanol reactor temperature of 220 °C, at atmospheric pressure and 70 bar, respectively. The reactor temperature of 220 °C was identified through a sensitivity analysis as the one that maximized the methanol output.

Table 4.3: Process Parameters

Parameter	**Value**
$LHV_{clean\ syngas}$ (MJ/kg)	15.31
LHV_{MeOH} (MJ/kg) [84][96]	19.9
Methanol productivity (kg/h)	9500
Methanol purity (%mol)	0.9926
Overall process energy efficiency (%)	0.45
CGE (%)	0.85
Carbon conversion efficiency (%)	0.41

4.3 Economic analysis

The total delivered equipment cost of each unit updated to 2024 is reported in Table 4.4. To obtain the total fixed capital cost, these values were summed up and multiplied by the overall installation factor for the complete system f_I, which resulted in 3.51.

Table 4.4: Total equipment purchased cost

Equipment	**Cost (M€$_{2024}$)**
MSW handling/ feeding	0.4402
Drier	0.4289
BFB autothermal gasifier	8.7892
Fabric filter	0.1368
RME scrubber	2.8031
SNG compressor	0.6761
Amine absorber	0.4206
ZnO guard bed	0.0016
WGS reactor	3.6103
Compressor to reactor	0.7607
Methanol reactor	3.7103
Distillation column	5.8765
ASU	9.3785
HX network	0.7341
Total	37.7671

Figure 4.1 shows the share of each unit to the total delivered equipment cost. The most expensive parts are the autothermal bubbling fluidized gasifier, including the ASU, representing around 48%, and the methanol loop, including the reactor, compressor, and distillation, accounting for around 37% of the total equipment costs. The high cost of the autothermal BFB and ASU unit can be attributed to the equipment complexity and the cutting-edge technology, respectively. These values have been compared to a similar work on waste gasification to methanol by Afzal et al. (2022) [85]. In their work, the gasification part accounts for 16% of the total, which differs greatly from this study. This discrepancy arises from the ASU not being included in their estimation. On the other hand, their methanol loop accounts for 47% of the total, which is similar to this project. The slight difference can be explained by a more rigorous model in the distillation that allowed for a better estimation.

Similar to the equipment costs, Figure 4.2 breaks down the share of each operating cost, which are also compared to those reported in Afzal et al. (2022) [85]. They reported that the catalyst and chemicals make up 7% of the total OPEX, similar to the 6.52% in this work. However, there are discrepancies in electricity costs: 23.96% in this project compared to 14% in their work. This difference can be attributed to the missing electricity consumption from the ASU unit in their analysis. For the remaining OPEX categories, Afzal et al. (2022) [85] do not pro-

vide a detailed breakdown like Figure 4.2. Additionally, while maintenance and taxes represent a significant portion of total OPEX, their values can vary greatly across different studies since they are calculated as a percentage of the capital cost.

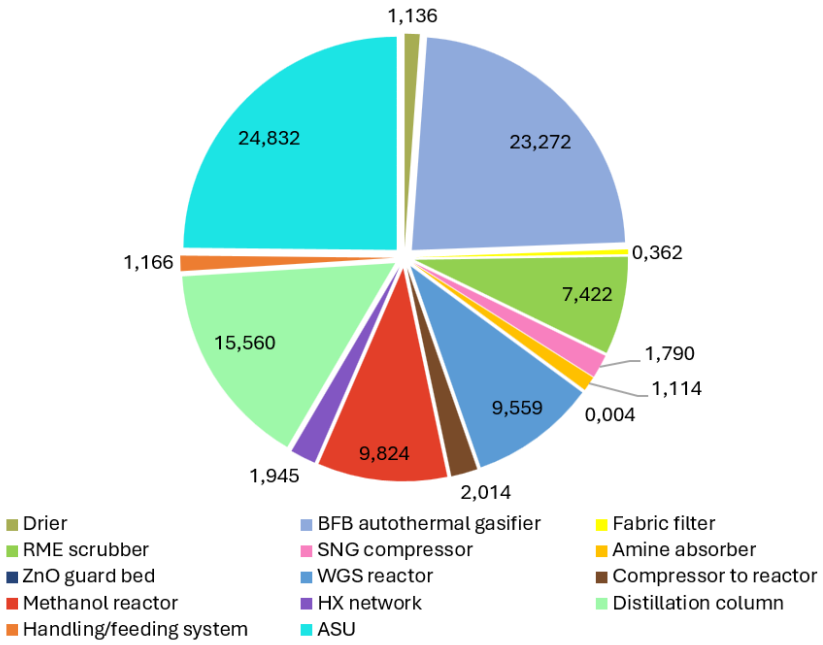

Figure 4.1: Share of equipment cost (%)

The economic indicators for the feasibility analysis are detailed in Table 4.5.
The project requires a substantial initial investment of 152.63 M€, including the 19.91 M€ of working capital needed to start the production. Despite this, the project is expected to recover the initial investment (break-even point) in roughly 5 years, with a strong return on the investment of 20.44%. Although this quick recovery (short PBP) is a good sign, it is insufficient to establish the profitability of the project, since it does not consider the time value of money. On the other hand, the NPV, which expresses the future cash flows discounted to their present value, is significantly high (276.28 M€), showing that the plant will likely be profitable in the long run.

The levelized cost of methanol is 414.92 €/tonne, which is competitive compared to the current market value for methanol of 450 €/tonne [82]. This is significantly lower than the cost of e-mehanol (950 €/tonne) produced from green hydrogen, obtained by water electrolysis using excess renewable electricity, and captured CO_2, separated from the flue gas of a conventional power station using an amine-based

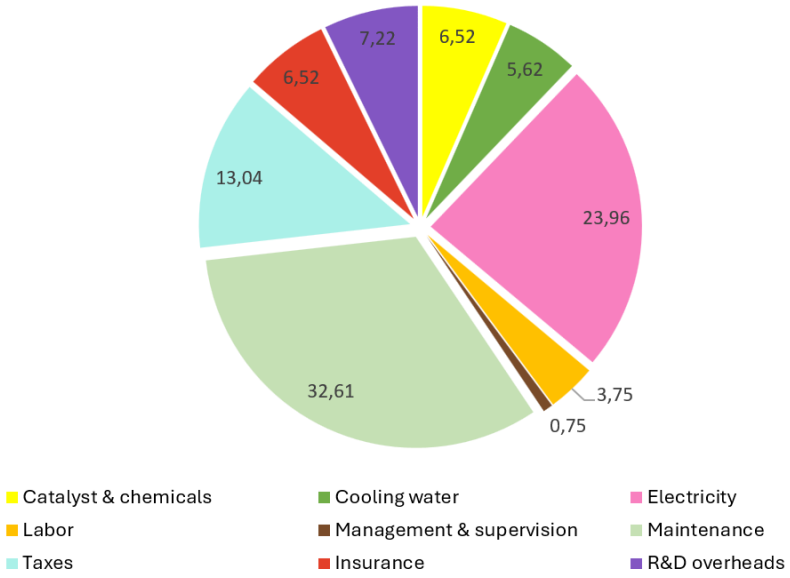

Figure 4.2: Share of operating cost (%)

absorption system [82]. The increasing demand for methanol may also support higher future prices, further enhancing the project´s competitiveness [82].

4.3.1 Sensitivity analysis

Following the economic analysis section, where the major cost contributors were identified, a sensitivity analysis was carried out on the levelized cost of methanol to explore potential areas for optimization.

This sensitivity analysis evaluates a 25% increase and decrease in the cost of each major contributor, recalculating the LCOM for each scenario. The results are shown in Figure 4.3, with the x-axis representing the percentage change in the original LCOM (414.92 €/tonne) when changing the parameter +25% or -25%. This shows that plant capacity has a major impact on process economics and efforts should be made to increase it. Moreover, although maintenance has a great impact in the LCoM as well, it was estimated as a percentage of the fixed capital cost according to literature, and therefore may not accurately reflect the actual maintenance requirements recommended by equipment suppliers.

Table 4.5: Economic parameters

Item	Value
Total fixed cost (M€$_{2024}$)	132.73
Working capital (M€$_{2024}$)	19.91
Total initial investment (M€$_{2024}$)	152.63
CRF	0.0802
Annualized capital cost (M€$_{2024}$/yr)	12.25
Annual operating cost (M€$_{2024}$/yr)	19.29
Annual revenue methanol (M€$_{2024}$/yr)	44.45
Annual revenue MSW (M€$_{2024}$/yr)	8.59
Total annual revenue (M€$_{2024}$/yr)	53.05
NPV (M€)	276.28
PBP (yrs)	5
ROI (%)	20.44
LCoM €/tonne	414.92

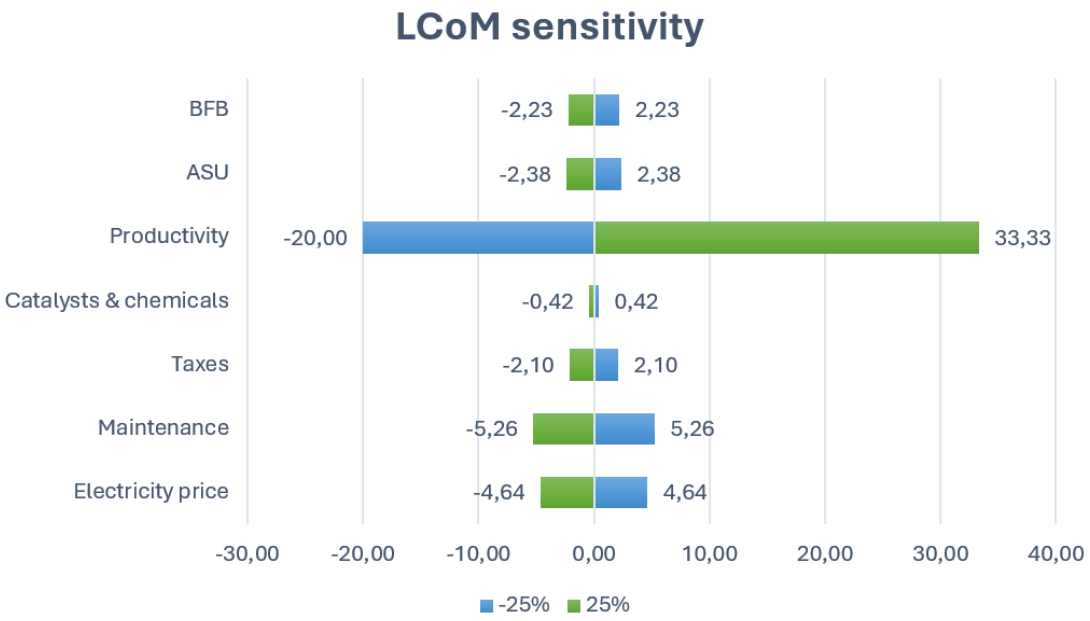

Figure 4.3: Sensitivity analysis on LCoM

5
Conclusion

This project presents a comprehensive review of the different gasification technologies available, as well as a compilation of several gasification commercial projects. By comparing these gasifiers regarding operating conditions, possible feedstock limitations, gasification agents, outlet gas composition, tar content in the gas, TRL, and other technological advantages and disadvantages, the Bubbling Fluidized Bed (BFB) proved to be the most suitable for handling diverse waste streams, thanks to its flexibility, thermal stability, and maturity. Additionally, methanol was selected over DME and ethanol as the product for the process for its versatility, and ultimately fewer additional steps, catalysts, and costs.

This work highlights the potential of Municipal Solid Waste gasification to produce methanol by developing a model in Aspen Plus followed by a techno-economic analysis. The model is designed for an input of 100 MW_{th} of MSW from Norway, with a moisture of 6.3%, and includes drying, gasification, syngas cleaning, syngas conditioning, methanol synthesis loop, and methanol purification stages. The BFB is modeled as an auto-thermal system, adjusting the inflow of oxygen to combust the volatile matter that releases the heat needed in the system. The gasifier operates at 920 °C so that the steam required in the process can be supplied by cooling the outlet gas. This part of the model was validated using the experimental values in Hejazi et al. (2017) [10]. After cleaning the syngas from particulate matter, tar, and acid gases, the ratio of H_2/CO is adjusted to meet the requirements needed for WtM processes. The kinetics of the CO and CO_2 hydrogenation, as well as the RWGS, are implemented in the synthesis reactor in Aspen plus, with an excess of Cu/Zn/Al/Zr catalyst, and the unconverted reactants are recycled to improve the conversion. The optimal temperature of the reactor was found to be 220 °C through a sensitivity analysis. The heating requirements for cold streams in the process are supplied by the hot streams throughout the process, with no surplus for district heating.

Moreover, a techno-economic analysis of this process was carried out, calculating the initial investment, annual cash flows, and different economic profitability in-

dicators. The BFB and the ASU are the major contributors to the capital cost of the process, while the electricity and maintenance are the major contributors to the costs needed to run and maintain the plant. For a plant capacity of 9500kg/h of methanol with a 99.3% molar purity, a substantial initial investment of 152.58 million EUR, expected to be recovered in 5 years with a strong ROI of 20.44%, and the OPEX is 19.29 MEUR annually. The NPV, which expresses the future cash flows discounted to their present value, is significantly high (276.28 M€), showing that the plant will likely be profitable in the long run. The levelized cost of methanol is 414.92 €/tonne, which is competitive compared to the current market value for methanol of 450 €/tonne [82][93], and significantly lower than the cost of e-methanol (950 €/tonne) [82][93]. The techno-economic analysis reveals promising financial indicators, including a high NPV and a competitive levelized cost of methanol, suggesting that the proposed process can be economically viable and competitive with current methanol production methods.

6
Future work

This project serves as the base for future research focusing on the following:

- **Optimization of the distillation column design in Aspen** → The methanol purification step is modelled with equilibrium stages, but a rigorous model can be implemented, optimizing the design, dimensions, and other parameters to get a more accurate representation of this step, improving the model and the economic analysis.
- **Exploration of addition of renewable hydrogen in the syngas conditioning step** → Assess the potential of green hydrogen as an alternative to the conventional WGS reactor when adjusting the H2/CO to meet the requirements for chemical synthesis. Compare this approach in terms of process complexity, costs, and sustainability.
- **Sensitivity analysis on feedstock water content** → Given the complexity and variability of MSW across regions, it would be useful to analyze how much this parameter influences the process efficiency and costs, although it would be expected to affect negatively with increasing moisture content.
- **Life Cycle Assessment (LCA) to explore greenhouse gas (GHG) emissions** → Assess the environmental impacts of this process and compare it to the conventional way of producing methanol and to the conventional waste incineration process. This will provide a better picture of the environmental benefits and potential trade-offs.

Bibliography

[1] S. M. Santos, A. C. Assis, L. Gomes, C. Nobre, and P. Brito, "Waste Gasification Technologies: A Brief Overview," *Waste*, vol. 1, no. 1, pp. 140–165, 12 2022.

[2] M. Niu, Y. Huang, B. Jin, and X. Wang, "Simulation of syngas production from municipal solid waste gasification in a bubbling fluidized bed using aspen plus," *Industrial and Engineering Chemistry Research*, vol. 52, no. 42, pp. 14 768–14 775, 10 2013.

[3] S. Mishra and R. K. Upadhyay, "Review on biomass gasification: Gasifiers, gasifying mediums, and operational parameters," *Materials Science for Energy Technologies*, vol. 4, pp. 329–340, 1 2021.

[4] J. Dai and K. J. Whitty, "Chemical looping gasification and sorption enhanced gasification of biomass: A perspective," *Chemical Engineering and Processing - Process Intensification*, vol. 174, 4 2022.

[5] A. Molino, S. Chianese, and D. Musmarra, "Biomass gasification technology-The state of the art overview," *Journal of Energy Chemistry*, vol. 25, no. 1, pp. 10–25, 1 2016.

[6] V. Palma, E. Meloni, C. Ruocco, M. Martino, and A. Ricca, "State of the Art of Conventional Reactors for Methanol Production," in *Methanol: Science and Engineering*. Elsevier, 2018, pp. 29–51.

[7] M. Sajid, A. Raheem, N. Ullah, M. Asim, M. S. Ur Rehman, and N. Ali, "Gasification of municipal solid waste: Progress, challenges, and prospects," *Renewable and Sustainable Energy Reviews*, vol. 168, 10 2022.

[8] S. Rudra and Y. K. Tesfagaber, "Future district heating plant integrated with municipal solid waste (MSW) gasification for hydrogen production," *Energy*, vol. 180, pp. 881–892, 8 2019.

[9] R. Smith, *Chemical Process Design and Integration*, 2nd ed. Chichester, West Sussex, United Kingdom: John Wiley & Sons, Inc, 2016.

[10] B. Hejazi, J. R. Grace, X. Bi, and A. Mahecha-Botero, "Kinetic Model of Steam Gasification of Biomass in a Dual Fluidized Bed Reactor: Comparison with Pilot-Plant Experimental Results," *Energy and Fuels*, vol. 31, no. 11, pp. 12 141–12 155, 11 2017.

[11] P. Chen, Q. Xie, M. Addy, W. Zhou, Y. Liu, Y. Wang, Y. Cheng, K. Li, and R. Ruan, "Utilization of Municipal Solid and Liquid Wastes for Bioenergy and Bioproducts Production," *ChemInform*, vol. 47, no. 30, 7 2016.

[12] A. Chanthakett, M. T. Arif, M. M. Khan, and A. M. Oo, "Performance assessment of gasification reactors for sustainable management of municipal solid waste," *Journal of Environmental Management*, vol. 291, 8 2021.

[13] U. Arena, "Process and technological aspects of municipal solid waste gasification. A review," *Waste Management*, vol. 32, no. 4, pp. 625–639, 4 2012.

[14] Avfall Sverige, "Swedish Waste Management 2022," Avfall Sverige, Tech. Rep., 7 2022.

[15] Z. Hameed, M. Aslam, Z. Khan, K. Maqsood, A. E. Atabani, M. Ghauri, M. S. Khurram, M. Rehan, and A. S. Nizami, "Gasification of municipal solid waste blends with biomass for energy production and resources recovery: Current status, hybrid technologies and innovative prospects," *Renewable and Sustainable Energy Reviews*, vol. 136, 2 2021.

[16] K. D. Sharma and S. Jain, "Municipal solid waste generation, composition, and management: the global scenario," *Social Responsibility Journal*, vol. 16, no. 6, pp. 917–948, 7 2020.

[17] L. Zhang, W. Wu, N. Siqu, T. Dekyi, and Y. Zhang, "Thermochemical catalytic-reforming conversion of municipal solid waste to hydrogen-rich synthesis gas via carbon supported catalysts," *Chemical Engineering Journal*, vol. 361, pp. 1617–1629, 4 2019.

[18] F. A. Lino, K. A. Ismail, and J. A. Castañeda-Ayarza, "Municipal solid waste treatment in Brazil: A comprehensive review," 9 2023.

[19] N. P. Cheremisinoff, "Municipal Solid Waste," in *Handbook of Solid Waste Management and Waste Minimization Technologies*, N. P. Cheremisinoff, Ed. Butterworth-Heinemann, 2003, ch. 3, pp. 34–95.

[20] J. Laso, I. García-Herrero, M. Margallo, A. Bala, P. Fullana-I-Palmer, A. Irabien, and R. Aldaco, "LCA-based comparison of two organic fraction municipal solid waste collection systems in historical centres in Spain," *Energies*, vol. 12, no. 7, 2019.

[21] S. E. Vergara and G. Tchobanoglous, "Municipal solid waste and the environment: A global perspective," pp. 277–309, 11 2012.

[22] A. Sandhi and J. Rosenlund, "Municipal solid waste management in Scandinavia and key factors for improved waste segregation: A review," 8 2024.

[23] Y. Sun and Y. Tang, "Municipal solid waste gasification integrated with water electrolysis technology for fuel production: A comparative analysis," *Chemical Engineering Research and Design*, vol. 191, pp. 14–26, 3 2023.

[24] L. Milios, "Municipal waste management in Sweden," European Environment Agency, Tech. Rep., 2 2013. [Online]. Available: http://www.cri.dk/

[25] S. B. Jones, Y. Zhu, and C. Valkenburg, "Municipal Solid Waste (MSW) to Liquid Fuels Synthesis, Volume 2: A Techno-economic Evaluation of the Production of Mixed Alcohols," Pacific Northwest National Laboratory, Richland, Tech. Rep., 4 2009. [Online]. Available: http://www.ntis.gov/ordering.htm

[26] A. Tremel, D. Becherer, S. Fendt, M. Gaderer, and H. Spliethoff, "Performance of entrained flow and fluidised bed biomass gasifiers on different scales," *Energy Conversion and Management*, vol. 69, pp. 95–106, 2013.

[27] T. Roshan Kumar, T. Mattisson, M. Rydén, and V. Stenberg, "Process Analysis of Chemical Looping Gasification of Biomass for Fischer-Tropsch Crude Production with Net-Negative CO2 Emissions: Part 1," *Energy and Fuels*, vol. 36, no. 17, pp. 9687–9705, 9 2022.

[28] N. M. Nguyen, F. Alobaid, P. Dieringer, and B. Epple, "Biomass-based chemical looping gasification: Overview and recent developments," 8 2021.

[29] Y. Wei, L. Cheng, B. Leckner, E. Wu, L. Li, and Q. Zhang, "Design of an industrial chemical looping gasification system," *Fuel*, vol. 330, 12 2022.

[30] S. Negi, G. Jaswal, K. Dass, K. Mazumder, S. Elumalai, and J. K. Roy, "Torrefaction: a sustainable method for transforming of agri-wastes to high energy density solids (biocoal)," *Reviews in Environmental Science and Biotechnology*, vol. 19, no. 2, pp. 463–488, 6 2020.

[31] C. Freda, E. Catizzone, A. Villone, and G. Cornacchia, "Biomass gasification in rotary kiln integrated with a producer gas thermal cleaning unit: An experimental investigation," *Results in Engineering*, vol. 21, 3 2024.

[32] C. Courson and K. Gallucci, "Gas cleaning for waste applications (syngas cleaning for catalytic synthetic natural gas synthesis)," in *Substitute Natural Gas from Waste: Technical Assessment and Industrial Applications of Biochemical and Thermochemical Processes*. Elsevier, 1 2019, pp. 161–220.

[33] G. Liu, H. Hagelin-Weaver, and B. Welt, "A Concise Review of Catalytic Synthesis of Methanol from Synthesis Gas," *Waste*, vol. 1, no. 1, pp. 228–248, 1 2023.

[34] P. K. Gupta, S. Datta, S. K. Saw, S. Kumari, G. Sahu, R. K. Singh, V. Chauhan, and P. D. Chavan, "Syngas Cleaning Technologies in Gasification Process for Downstream Applications," in *Proceedings of the 10th Asian Mining Congress 2023. AMC 2023. Springer Proceedings in Earth and Environmental Sciences*, A. Sinha, B. C. Sarkar, and P. K. Mandal, Eds. Springer, 2023, pp. 307–316.

[35] P. J. Woolcock and R. C. Brown, "A review of cleaning technologies for biomass-derived syngas," pp. 54–84, 5 2013.

[36] N. Abdoulmoumine, S. Adhikari, A. Kulkarni, and S. Chattanathan, "A review on biomass gasification syngas cleanup," pp. 294–307, 10 2015.

[37] R. Zwart, S. Van Der Heijden, R. Emmen, J. Dall Bentzen, J. Ahrenfeldt, P. Stoholm, and J. Krogh, "Tar removal from low-temperature gasifiers," Energy Research Centre of the Netherlands (ECN). ECN-E-10-008, Tech. Rep., 4 2010. [Online]. Available: http://www.ecn.nl/docs/library/report/2010/e10008.pdf

[38] C. Frilund, S. Tuomi, E. Kurkela, and P. Simell, "Small- to medium-scale deep syngas purification: Biomass-to-liquids multi-contaminant removal demonstration," *Biomass and Bioenergy*, vol. 148, 5 2021.

[39] M. D. Kaufman Rechulski, T. J. Schildhauer, S. M. Biollaz, and C. Ludwig, "Sulfur containing organic compounds in the raw producer gas of wood and grass gasification," *Fuel*, vol. 128, pp. 330–339, 7 2014.

[40] P. Mondal, G. S. Dang, and M. O. Garg, "Syngas production through gasification and cleanup for downstream applications - Recent developments," *Fuel Processing Technology*, vol. 92, no. 8, pp. 1395–1410, 2011.

[41] M. Puig-Gamero, J. Argudo-Santamaria, J. L. Valverde, P. Sánchez, and L. Sanchez-Silva, "Three integrated process simulation using aspen plus®: Pine gasification, syngas cleaning and methanol synthesis," *Energy Conversion and Management*, vol. 177, pp. 416–427, 12 2018.

[42] A. M. Ribeiro, J. C. Santos, and A. E. Rodrigues, "PSA design for stoichiometric adjustment of bio-syngas for methanol production and co-capture of carbon dioxide," *Chemical Engineering Journal*, vol. 163, no. 3, pp. 355–363, 10 2010.

[43] S. Ghosh, V. Uday, A. Giri, and S. Srinivas, "Biogas to methanol: A comparison of conversion processes involving direct carbon dioxide hydrogenation and via reverse water gas shift reaction," *Journal of Cleaner Production*, vol. 217, pp. 615–626, 4 2019.

[44] A. Giuliano, C. Freda, and E. Catizzone, "Techno-economic assessment of bio-syngas production for methanol synthesis: A focus on the water–gas shift and carbon capture sections," *Bioengineering*, vol. 7, no. 3, pp. 1–18, 7 2020.

[45] M. Shahrivar, M. Nauman Saeed, G. D. Surywanshi, T. Mattisson, and A. H. Soleimanisalim, "Improving bio aviation fuel yield from biogenic carbon sources through electrolysis assisted chemical looping gasification," *Fuel*, vol. 348, 9 2023.

[46] S. Sepahi and M. R. Rahimpour, "Methanol production from syngas," in *Advances in Synthesis Gas: Methods, Technologies and Applications: Volume 3: Syngas Products and Usages*. Elsevier, 1 2022, pp. 111–146.

[47] F. Nestler, A. R. Schütze, M. Ouda, M. J. Hadrich, A. Schaadt, S. Bajohr, and T. Kolb, "Kinetic modelling of methanol synthesis over commercial catalysts: A critical assessment," *Chemical Engineering Journal*, vol. 394, 8 2020.

[48] F. J. Gutiérrez Ortiz, A. Serrera, S. Galera, and P. Ollero, "Methanol synthesis from syngas obtained by supercritical water reforming of glycerol," *Fuel*, vol. 105, pp. 739–751, 3 2013.

[49] R. Timsina, R. K. Thapa, B. M. E. Moldestad, and M. S. Eikeland, "Methanol Synthesis from Syngas: a Process Simulation," in *Proceedings of The First SIMS EUROSIM Conference on Modelling and Simulation, SIMS EUROSIM 2021, and 62nd International Conference of Scandinavian Simulation Society, SIMS 2021, September 21-23, Virtual Conference, Finland*, vol. 185. Linköping University Electronic Press, 3 2022, pp. 444–449.

[50] J. Toyir, R. Miloua, N. E. Elkadri, M. Nawdali, H. Toufik, F. Miloua, and M. Saito, "Sustainable process for the production of methanol from CO2 and H2 using Cu/ZnO-based multicomponent catalyst," *Physics Procedia*, vol. 2, no. 3, pp. 1075–1079, 11 2009.

[51] F. Dalena, A. Senatore, M. Basile, S. Knani, A. Basile, and A. Iulianelli, "Advances in methanol production and utilization, with particular emphasis toward hydrogen generation via membrane reactor technology," 12 2018.

[52] Vesterinen Eero, "Methanol Production via CO2 Hydrogenation," Aalto University School of Engineering, Espoo, Tech. Rep., 11 2018.

[53] K. Qadeer, A. Al-Hinai, L. F. Chuah, N. R. Sial, A. H. Al-Muhtaseb, R. Al-Abri, M. A. Qyyum, and M. Lee, "Methanol production and purification via membrane-based technology: Recent advancements, challenges and the way forward," *Chemosphere*, vol. 335, 9 2023.

[54] X. Cui and S. K. Kær, "A comparative study on three reactor types for methanol synthesis from syngas and CO2," *Chemical Engineering Journal*, vol. 393, 8 2020.

[55] A. A. Kiss, J. J. Pragt, H. J. Vos, G. Bargeman, and M. T. de Groot, "Novel efficient process for methanol synthesis by CO2 hydrogenation," *Chemical Engineering Journal*, vol. 284, pp. 260–269, 1 2016.

[56] M. Shahrivar and M. Nauman Saeed, "Chemical-looping gasification for the production of aviation fuel with negative emissions: Full chain process modeling and techno-economic analysis," Ph.D. dissertation, Chalmers University of Technology, Göteborg, 2022. [Online]. Available: www.chalmers.seShutterstock

[57] S. S. Hla and D. Roberts, "Characterisation of chemical composition and energy content of green waste and municipal solid waste from Greater Brisbane, Australia," *Waste Management*, vol. 41, pp. 12–19, 7 2015.

[58] Aspen Technology, "Getting Started Modeling Processes with Solids Aspen Plus," Aspen Technology, Burlington, MA, Tech. Rep., 2013. [Online]. Available: http://www.aspentech.com

[59] M. Arvidsson, M. Morandin, and S. Harvey, "Biomass gasification-based syngas production for a conventional oxo synthesis plant-process modeling, integration opportunities, and thermodynamic performance," *Energy and Fuels*, vol. 28, no. 6, pp. 4075–4087, 6 2014.

[60] F. Ju, H. Chen, X. Ding, H. Yang, X. Wang, S. Zhang, and Z. Dai, "Process simulation of single-step dimethyl ether production via biomass gasification," *Biotechnology Advances*, vol. 27, no. 5, pp. 599–605, 9 2009.

[61] S. hyun Kim, Y. don Yoo, J. Hoi Gu, and M. Hyun Kim, "Water Gas Shift Reaction Characteristics Using Syngas from Waste Gasification," *International Journal of Engineering Science Invention*, vol. 6, no. 5, pp. 35–43, 5 2017. [Online]. Available: www.ijesi.org||Volumewww.ijesi.org

[62] S. Van-Dal and C. Bouallou, "Design and simulation of a methanol production plant from CO2 hydrogenation," *Journal of Cleaner Production*, vol. 57, pp. 38–45, 10 2013.

[63] T. Roshan Kumar, T. Mattisson, and M. Rydén, "Techno-Economic Assessment of Chemical Looping Gasification of Biomass for Fischer-Tropsch Crude Production with Net-Negative CO2Emissions: Part 2," *Energy and Fuels*, 2022.

[64] M. N. Saeed, M. Shahrivar, G. D. Surywanshi, T. R. Kumar, T. Mattisson, and A. H. Soleimanisalim, "Production of aviation fuel with negative emissions via chemical looping gasification of biogenic residues: Full chain process modelling and techno-economic analysis," *Fuel Processing Technology*, vol. 241, 3 2023.

[65] A. R. Ahmadi, M. R. Rahimpour, and M. Farsi, "Efficient recycling and conversion of CO2 to methanol: Process design and environmental assessment," *Chemical Engineering Research and Design*, vol. 202, pp. 403–413, 2 2024.

[66] R. M. Swanson, J. A. Satrio, R. C. Brown, A. Platon, and D. D. Hsu, "Techno-Economic Analysis of Biofuels Production Based on Gasification," Tech. Rep., 2010. [Online]. Available: http://www.osti.gov/bridge

[67] Exchange Rates, "US Dollar (USD) To Euro (EUR) Exchange Rate History for 2024." [Online]. Available: https://www.exchange-rates.org/exchange-rate-history/usd-eur-2024

[68] C. Maxwell, "Cost Indices," 4 2024. [Online]. Available: https://toweringskills.com/financial-analysis/cost-indices/

[69] C. N. Hamelinck, A. P. Faaij, H. den Uil, and H. Boerrigter, "Production of FT transportation fuels from biomass; technical options, process analysis and optimisation, and development potential," *Energy*, vol. 29, no. 11, pp. 1743–1771, 2004.

[70] S. Heyne and S. Harvey, "Impact of choice of CO2 separation technology on thermo-economic performance of Bio-SNG production processes," *Interna-*

tional Journal of Energy Research, vol. 38, no. 3, pp. 299–318, 3 2014.

[71] C. N. Hamelinck and A. P. C. Faaij, "Future prospects for production of methanol and hydrogen from biomass," *Journal of Power Sources*, vol. 111, no. 1, pp. 1–22, 2002.

[72] Y. Gu, D. Wang, Q. Chen, and Z. Tang, "Techno-economic analysis of green methanol plant with optimal design of renewable hydrogen production: A case study in China," *International Journal of Hydrogen Energy*, vol. 47, no. 8, pp. 5085–5100, 1 2022.

[73] G. Towler and R. Sinnott, "Estimating Revenues and Production Costs," in *Chemical Engineering Design*. Elsevier, 2013, pp. 355–387.

[74] I. Hannula, "Hydrogen enhancement potential of synthetic biofuels manufacture in the European context: A techno-economic assessment," *Energy*, vol. 104, pp. 199–212, 6 2016.

[75] Y. A. Alsultanny and N. N. Al-Shammari, "Oxygen specific power consumption comparison for air separation units," *Engineering Journal*, vol. 18, no. 2, pp. 67–80, 4 2014.

[76] INTRATEC, "Cooling Water Cost - Industrial Utilities." [Online]. Available: https://www.intratec.us/products/water-utility-costs/commodity/cooling-water-cost

[77] Konsumenternas Energimarknadsbyrå, "Månadspriser på elbörsen [Monthly Prices on the Electricity Exchange]." [Online]. Available: https://www.energimarknadsbyran.se/el/dina-avtal-och-kostnader/elpriser-statistik/manadspriser-pa-elborsen/

[78] M. Scomazzon, E. Barbera, and F. Bezzo, "Alternative sustainable routes to methanol production: Techno-economic and environmental assessment," *Journal of Environmental Chemical Engineering*, vol. 12, no. 3, 6 2024.

[79] The Methanol Insitute, "Methanol Price and Supply/ Demand." [Online]. Available: https://www.methanol.org/methanol-price-supply-demand/

[80] D. Hogg, "Costs for Municipal Waste Management in the EU-Final Report to Directorate General Environment,
}European Commission," Eunomia Research & Consulting, Tech. Rep.

[81] G. Towler and R. Sinnott, "Economic Evaluation of Projects," in *Chemical Engineering Design*. Elsevier, 2013, pp. 389–429.

[82] S. Sollai, A. Porcu, V. Tola, F. Ferrara, and A. Pettinau, "Renewable methanol production from green hydrogen and captured CO2: A techno-economic assessment," *Journal of CO2 Utilization*, vol. 68, 2 2023.

[83] L. Muriuki, D. Wafula Wekesa, and F. Njoka, "Modeling, simulation and techno-economic evaluation of a micro-grid system based on steam gasification of organic municipal solid waste," *Energy Conversion and Management*, vol. 299, 1 2024.

[84] Methanol Institute, "Physical properties of pure methanol." [Online]. Available: https://www.methanol.org/wp-content/uploads/2016/06/Physical-Properties-of-Pure-Methanol.pdf

[85] S. Afzal, A. Singh, S. R. Nicholson, and G. T. Beckham, "Techno-Economic Analysis of Municipal Solid Waste Gasification to Methanol," Tech. Rep. [Online]. Available: https://www.nrel.gov/manufacturing/mfi-modeling-tool.html

[86] O. Condori, F. García-Labiano, L. F. de Diego, M. T. Izquierdo, A. Abad, and J. Adánez, "Biomass chemical looping gasification for syngas production using ilmenite as oxygen carrier in a 1.5 kWth unit," *Chemical Engineering Journal*, vol. 405, 2 2021.

[87] L. Waldheim and Waldheim Consulting, "Gasification of waste for energy carriers- A review," IEA Bioenergy, Tech. Rep., 2018.

[88] Y. Jafri, L. Waldheim, W. Consulting, and J. Lundgren, "Emerging Gasification Technologies for Waste & Biomass," IEA Bioenergy, Tech. Rep., 12 2020.

[89] B. Wang, R. Gupta, L. Bei, Q. Wan, and L. Sun, "A review on gasification of municipal solid waste (MSW): Syngas production, tar formation, mineral transformation and industrial challenges," pp. 26 676–26 706, 8 2023.

[90] M. T. Hansen and I. S. Christiansen, "Thermal Biomass Gasification in Denmark - IEA Bioenergy Task 33 Country Report," IEA Bioenergy, Tech. Rep., 2019. [Online]. Available: https://task33.ieabioenergy.com/wp-content/uploads/sites/33/2022/06/Danish-Coutry-Report-2019-final.pdf

[91] Power Technology, "Energy Works Power Plant Project, Hull," 4 2016. [Online]. Available: https://www.power-technology.com/projects/energy-works-power-plant-project-hull/?cf-view

[92] K. Ståhl and M. Neergaard, "IGCC Power plant for biomass utilisation, Värnamo, Sweden," *Biomass and Bioenergy*, vol. 15, no. 3, pp. 205–211, 1998.

[93] Dall Energy, "EUDP Demonstration Project Final Report - Sustainable Biomass Heat & Power in Sindal, Denmark," Dall Energy, Hørsholm, Tech. Rep., 5 2019. [Online]. Available: https://energiforskning.dk/sites/energiforskning.dk/files/slutrapporter/sindal_-_eudp_slutrapport_2019-05-09.pdf

[94] Energy Works, "Energy Works Hull Technology." [Online]. Available: http://energyworkshull.co.uk/technology/

[95] J. Hrbek, "Status report on thermal gasification of biomass and waste 2021 Annex 5 Other gasification technology-operational/commissioning/erection/planned," IEA Bioenergy, Tech. Rep.,

2021. [Online]. Available: https://task33.ieabioenergy.com/wp-content/uploads/sites/33/2022/07/Other-technology-oper-final.pdf

[96] ECN, "MILENA Biomass Gasification Process," 12 2011. [Online]. Available: https://www.milenatechnology.com/

[97] C. M. Van Der Meijden, "Development of the MILENA gasification technology for the production of Bio-SNG," Ph.D. dissertation, Eindhoven University of Technology, Eindhoven, 12 2010.

[98] N. Kokel, "Technology units- Ebara UBE Process," 9 2023. [Online]. Available: https://portfolio-pplus.com/Technologies/Details/232

[99] Ebara, "Gasification technologies." [Online]. Available: https://www.eep.ebara.com/en/business_technology/technology_3.html

[100] Babcock Steinmüller Environment, "Waste gasification - Direct Melting System," Tech. Rep. [Online]. Available: https://www.hzi-steinmueller.com/wp-content/uploads/downloads/broschure-waste-gasification-en.pdf

[101] M. A. Satiada and A. Calderon, "Comparative analysis of existing waste-to-energy reference plants for municipal solid waste," *Cleaner Environmental Systems*, vol. 3, 12 2021.

[102] O. Condori, F. García-Labiano, L. F. De Diego, M. T. Izquierdo, A. Abad, and J. Adánez, "Syngas production via Biomass Chemical Looping Gasification (BCLG) in a 50 kW th unit using ilmenite as oxygen carrier," in *Fluidized Bed Conversion Conference*, 5 2022.

[103] F. Marx, P. Dieringer, J. Ströhle, C. Linderholm, N. Detsios, K. Atsonios, C. Aichernig, T. Liese, F. Buschsieweke, Y. Huang, and N. Gürer, "Chemical Looping Gasification for Sustainable Production of Biofuels Public Report IV," European Union's Horizon 2020, Tech. Rep., 6 2023. [Online]. Available: https://clara-h2020.eu/public-reports/

[104] M. Shahabuddin, M. T. Alam, B. B. Krishna, T. Bhaskar, and G. Perkins, "A review on the production of renewable aviation fuels from the gasification of biomass and residual wastes," 9 2020.

[105] J. Hrbek, "Status report on thermal gasification of biomass and waste 2021 Annex 3 Gasification facilities for fuel synthesis-planned, under construction, under commissioning, operational," IEA Bioenergy, Tech. Rep., 2021.

[106] ——, "Status report on thermal gasification of bimass and waste 2019 Annex 1 Gasification facilities for CHP production-operational, under construction, under commissioning," IEA Bioenergy, Tech. Rep., 2019. [Online]. Available: http://burkhardt-energy.com/hp538/Technik.htm

[107] C. A. Jordan, J. Weatherby, and A. Barclay, "Advanced Gasification Technologies – Review and Benchmarking: Review of current status of advanced gasification technologies," 10 2021. [Online]. Available: https:

//assets.publishing.service.gov.uk/government/uploads/system/uploads/attachment_data/file/1023792/agt-benchmarking-task-2-report.pdf

[108] L. E. Lücking, "Methanol Production from Syngas Process modelling and design utilising biomass gasification and integrating hydrogen supply," Ph.D. dissertation, Delft University of Technology, Delft, 12 2017. [Online]. Available: http://repository.tudelft.nl/.

[109] P. Tuna, "Generation of synthesis gas for fuels and chemicals production," Ph.D. dissertation, Lund University, Lund, 2013.

[110] Methanex, "Methanex Methanol Price Sheet," 1 2024. [Online]. Available: https://www.methanex.com/wp-content/uploads/Mx-Price-Sheet-January-30-2024.pdf

[111] G. Iaquaniello, G. Centi, A. Salladini, E. Palo, S. Perathoner, and L. Spadaccini, "Waste-to-methanol: Process and economics assessment," *Bioresource Technology*, vol. 243, pp. 611–619, 2017.

[112] Market Observatory for Energy DG Energy, "Quarterly report On European gas markets," Market Observatory for Energy of the European Commission, Tech. Rep., 2023. [Online]. Available: https://energy.ec.europa.eu/system/files/2023-12/New_Quarterly_Report_on_European_Gas_markets_Q2_2023.pdf

[113] D. Katla-Milewska, S. M. Nazir, and A. Skorek-Osikowska, "Synthetic natural gas (SNG) production with higher carbon recovery from biomass: Techno-economic assessment," *Energy Conversion and Management*, vol. 300, 1 2024.

[114] Mike, "Dimethyl Ether Price Index," 2 2024. [Online]. Available: https://businessanalytiq.com/procurementanalytics/index/dimethyl-ether-price-index/

[115] D. M. Kennes-Veiga, C. Fernández-Blanco, M. C. Veiga, and C. Kennes, "Ethanol production from syngas," in *Advances in Synthesis Gas: Methods, Technologies and Applications: Volume 3: Syngas Products and Usages*. Elsevier, 1 2022, pp. 147–171.

[116] "Ethanol prices," 2 2024. [Online]. Available: https://www.globalpetrolprices.com/ethanol_prices/

[117] S. Phillips, A. Aden, J. Jechura, D. Dayton, and T. Eggeman, "Thermochemical Ethanol via Indirect Gasification and Mixed Alcohol Synthesis of Lignocellulosic Biomass," Tech. Rep., 2012. [Online]. Available: http://www.osti.gov/bridge

A

Appendix 1

Table A.1: Gasification technologies

Reactor type	T [°C]	P [bar]	Residence time	Feedstock limitations	Pre-treatment	Input	Gasif. agent	LHV output (MJ/Nm^3)	Gas composition (vol.%, db)	Tar content in gas (g/Nm^3)	Particles in gas (% db)	TRL (*)	Utility needed	Advantages	Disadvantages
Updraft (or counter current) fixed bed	500-1200	1-100	900-1800 s	Moisture < 50% Particle size ≤100 mm Bulk density >400 kg/m^3	Yes, size homogenization	MSW	Steam	4.5-5	CO: 11-23 CO_2: 21-38 H_2: 34-54 CH_4: 1-10 N_2: –	>10	<15	6-7	Preheated air	- High thermal efficiency - Simple design and construction - Suitable for a wide range of moisture content and size - High gasification efficiency - Robust and reliable technology	- Temperature gradients and hot spots, difficult temperature control - Limited process flexibility - Need for uniform feedstock size - High tar content in the syngas - Low CO and H_2 content in the syngas, requiring subsequent treatment
Downdraft (or co-current) fixed bed	500-1200	1-100	900-1800 s	Moisture < 20% Particle size ≤100 mm Bulk density >500 kg/m^3	Yes, size homogenization	MSW and biomass	Air	4-6	CO: 13-18 CO_2: 12-16 H_2: 11-16 CH_4: 2-6 N_2: 45-60	<1	<5	6-7	Preheated air	- Low tar production - Simple design and construction - High carbon conversion - Limited entrainment of ash and dust - Reliable and low-cost process	- Requirement of feedstock with low moisture content - Limited process flexibility - Difficulty in controlling the heat in the reactor
Bubbling fluidized bed (BFB)	800-1000	1-30	Minutes to hours	Moisture < 55% Particle size ≤100 mm	Yes/No Drying might be needed Bulk density >100 kg/m^3	MSW and biomass	Steam	12-14	CO: 25-30 CO_2: 20-25 H_2: 35-40 CH_4: 9-11 N_2: 0-5	>10	<25	8-9	Superheated steam, cooling water	- High carbon conversion - Good mixing and gas-solid contact - Good temperature control - Low tar production Good tolerance with heterogeneous feedstock and higher moisture content	- Requirement of pretreatment of heterogeneous feedstock - Restrictions on the bed and feed size - Risk of fluidization of the bed at high T - Entrainment of dust and ashes High investment and maintenance costs
Circulating fluidized bed (CFB)	700-1000	1-30	Minutes to hours	Moisture < 55% Particle size ≤100 mm Bulk density >100 kg/m^3	Yes, Pulverization	MSW	Steam	12-14	CO: 15-19 CO_2: 17-18 H_2: 7-10 CH_4: 3 N_2: –	>10	<25	8-9	Hot bed	- High carbon conversion - Low tar production -Good tolerance with heterogeneous feedstock and higher moisture content - Very good scale-up	-High pressure drop - Complex operation and process control problems -High investment - Loss of carbon in the ashes - Pretreatment of the feedstock is needed

Continued on next page

Table A.1 – *Continued from previous page*

Reactor type	T [°C]	P [bar]	Residence time	Feedstock limitations	Pre-treatment	Input	Gasif. agent	LHV output (MJ/Nm^3)	Gas composition (vol.%, db)	Tar content in gas (g/Nm^3)	Particles in gas (% db)	TRL (*)	Utility needed	Advantages	Disadvantages
Chemical looping (CLG): DIFB- an Air Reactor (AR) and Fuel Reactor (FR)	AR: 700-950 FR: 700-950	1-10	Minutes to hours	Particle size < 200-1000 μ if volatiles content > 25-37 wt.% Particle size < 90-200 μ if volatiles content < 10 wt.%	Yes, drying, desnification, grinding, torrefaction	Biomass	Steam, metal oxides (Me_xO_y) as oxygen carriers (OC) i.e LD slag, ilmenite	19.34 (feedstock)	CO: 42.4 CO_2: 16.9 H_2: 27.2 CH_4: 10.1 C_{2-3} 3.4 N_2: – At 940 °C, with S/B of 0.6 kg/kg and OB λ of 0.34	2-15	-	5-6	-	- Oxygen carrier tranfers both oxygen and heat from the AR to the FR -Catalytic action of metal oxides can reduce significantly tar formation - Nitrogen free syngas product -High carbon conversion is possible	-Novel technology -System complexity -Challenge to minimize the loss of the looping materials - Susceptibility to equipment corrosion due to biomass composition - Clogging and blockages due to tar compounds -Extensive criteria for selecting a successful OC
Entrained flow bed	1200-1500	20-80	1-5s	Moisture < 15% Particle size ≤1 mm Bulk density >400 kg/m^3	Yes, torrefaction/HTC	MSW and biomass	Air, O_2	10-12	CO: 45-55 CO_2: 10-15 H_2: 23-28 CH_4: 0-1 N_2: 0-1	«1	<20	6-7	Cooling water	- High carbon conversion - Uniform temperature - Very low tar production - Feedstock flexibility -Good process control -Vitrified slag	- Feedstock size and moisture content restrictions -Large oxidant requirements -Heat recovery is required to improve efficiency -Feedstock pretreatment is necessary -High investment and operational costs
Rotary kiln	300-600	20-80	1-2 hours	No problem with moisture Flexible particle size Bulk density >100 kg/m^3	No	RDF and biomass	Steam	12	CO: 2.2-16.8 CO_2: 20.1-25.3 H_2: 59.1-66.9 CH_4: 3-5.6 N_2: –	-	<45	5-6	Heating gas	-Feedstock flexibility in composition, size, and moisture content -High carbon conversion -Simple operation - Low investment costs	-Problems in starting-up and controlling the temperature -High energy consumption - High production of dust and tar - Low heat exchange capacity -High maintenance costs
Plasma	1400-2000 Plasma torch at 1000	1-30	Minutes to hours	No problem with moisture Flexible particle size Bulk density >100 kg/m^3	No	MSW	Air, O_2, steam	6-7	CO: 42.9 CO_2: 16.6 H_2: 34.8 CH_4: 0.1 N_2: 5.6	<1	<20	5-6	-	-No pretreatment requirement -Vitrified slag, from which non-leachable products can be recovered -High syngas yields - Low energy loss	-Very high energy consumption -Safety problems -Non continuous process - Thermal shock in start- up and shut down -High operational and maintenance costs

Source: Adapted from [12], [13], [1], [86], [7], [26], [27], [4], [28], [29], [87].

Table A.2: Gasification Projects Overview

Company/ Project	Country	Gasification technology	Feedstock	Gasification agent	Final product	TRL	Other characteristics
Enerkem Alberta Biofuels LP/ Edmonton Waste-to-Biofuels	Canada	BFB	Sorted MSW (dry)	Air and steam	Methanol, ethanol	8-9	P: up to 16 atm; T: 700-750°C
Ebara Environmental Plant UBE Industries/ Ebara UBE Process	Japan	Pressurized twin Internally circulating fluidized-bed (PTICFG) and ash melting system	Pretreated MSW	Steam, air, oxygen	Hydrogen gas - NH_3	9	Low T gasification (600-800°C) coupled with high T slagging gasification (1300-1500°C)
ECN/ MILENA Gasifier	The Nether-lands	MILENA BFB (pressurized, allothermal)	Wood, sewage sludge, lignite	Steam, air	SNG, electricity	4-5	T: 850°C; Bed materials: olivine, dolomite, and sand; Patented technology; Tar free syngas (OLGA tar removal)
Energy Works/ Energy Works Hull Power Plant	UK	FB	Waste wood, SRF, MSW	Staged air	CHP-electricity $28MW_{el}$, biomethane $3MW_{th}$	8	Multiple feedstocks blended; T: 700-930°C
Nippon Steel Engineering/ Shin-Moji Plant	Japan	Downdraft- Direct Melting System (DMS)	MSW, incombustible residues (IR)	Oxygen enriched air (36% O_2)	Energy production 23.5 MW	9	T:400-1700°C; P: atmospheric; Granulated slag; Ferrous metal recovery; No feedstock pretreatment
COGENT ENERGY	USA	Plasma	MSW, ISW	Air	CHP electricity, liquid fuels, and H_2	5-6	Small scale; Capacity: 365-1825 tons/ year
ICB-CSIC/ EU Horizon 2020 CLARA Project	Spain	BCLG	Wheat straw pellets	Ilmenite as oxygen carrier	Syngas	4-5	T: 980°C; Tests to optimize the design and operating conditions of CLG; Ilmenite has low agglomeration tendency; Steam-to-biomass ratio of 0.7 kg/kg dry biomass in the FR
Advanced Biofuel Solutions Ltd/ RadGas Technology	UK	BFB	RDF	Oxygen, steam	BioSNG, CO_2, vitrified ash	6	High T plasma converter for syngas contaminants' removal
SUNY Cobleskill/ Caribou Biofuels	USA	Rotary kiln	Unprocessed MSW	Air	Power, biofuel, and biochar	5-6	Moisture content in feedstock can exceed 80%; Optimized rotation rate for enhanced char conversion

Continued on next page

Table A.2: Gasification Projects Overview (continued)

Company/ Project	Country	Gasification technology	Feedstock	Gasification agent	Final product	TRL	Other characteristics
ThermoChem Recovery International (TRI)/ Fully Integrated BioRefinery	USA	FB	Organic residues and waste streams	Steam	FT liquids	6-7	Indirect heat supplied by high T flue gas passing through internal tubes; Bed material Al_2O_3; Particulate removal integrated within the gasifier
MEVA Energy AB/ MEVA Technology	Sweden	Entrained flow cyclone	Crushed pellets, sawdust	Air	CHP, biochar	7-8	T: 800-1000°C; TRL: 8; Two step syngas cleaning: venture scrubber and wet electrostatic precipitator
Lahti Energia Oy/ Kymijärvi II	Finland	CFB	SRF	Oxygen and air	Electricity and heat	9	T: 850-900°C; P: atmospheric; Bed of sand and lime particles; Moisture content of SRF: 15-25%
Kew Technology	UK	BFB	RDF, hazardous waste	Oxygen / air/ steam	H_2 rich syngas	6	T: 800°C; P: 7 bar
GoBiGas	Sweden	Dual FB (CFB combustor and BFB gasifier)	Forest residues	Steam	Biomethane	8	T:700-800°C; P: atmospheric; Moisture content < 20 wt%; Biomethane compliant with European Standard for injection into the natural gas grid
PowerHouse Energy/ Distributed Modular Gasification Technology (DMG®)	UK	Pressurized rotary kiln	Mixed plastics, RDF and SRF	Superheated steam	Hydrogen and electricity	6	T> 850°C
Sindal District Heating Company/ Dall Energy CHP Sindal	Denmark	Updraft fixed bed	Wood chips, green wood waste	Staged air	CHP	8	Moisture in fuel 20-60%; C content in bottom ash < 1%
Sumitomo SHI FW/ NSE Biofuels Oy	Finland	CFB	Biomass and waste derived fuels	Steam and O_2	FT liquids, renewable diesel	7	T: 830-940°C; Steam supplied by a waste heat boiler; Oxygen supplied by an ASU
Växamo Plant	Sweden	CFB	Wood chips	Air	IGCC	9	P: 20 bar; T: 950-1000°C; Pretreatment: drying

Continued on next page

Source: Adapted from [1], [88], [89], [90], [91], [92], [93], [94], [95], [96],[97], [98], [99],[100], [101], [102], [103], [104], [105], [106], [107].

Table A.3: Chemical synthesis

Product	Feedstock	P (bar)	T (°C)	Ratio	Utility needed	Catalyst	TRL	Production price	Market price	Refs
Methanol	Syngas	Low P: 50-100; High P: 240-300	Low P: 240-260; High P: 350-400	CO_2/CO:H_2 2/28:70	Superheated steam	Cu/ZnO/Al_2O_3, Cu/ZnO/Cr_2O_3	9	110€/MT for a new WtM 300 MT/d plant, using RDF as feedstock and O_2 as gasification agent in a HT gasifier (fixed bed). Quenching, desulfurization, WGS reactor and methanol synthesis reactor	525 €/ MT (metric ton)	[87], [108], [109], [110], [111]
SNG (Bio-methane)	Syngas	10-50	250-300	H_2/CO=3.1	Cooling water	-	6-7	58€/MWh Indirect steam-blown dual fluidized bed biomass gasifier, syngas fixed-bed methanation, and additional source of H_2 (water electrolysis)	35.2€/MWh	[32], [112], [113]
DME	Methanol	10-20	300-240	-	Steam	Strong acidic catalyst like Al_2O_3, or zeolites	5-6	653.9 USD/MT Methanol dehydration in γ-Al_2O_3. Syngas from MSW gasification at 2 MPa and 968 °C	0.88 USD/kg (Europe)	[23], [109], [114]
Ethanol	Methanol	15-80	350	H_2/CO=2	Steam	Cu/ZnO/Al_2O_3, Cu/ZnO/Mg_2O_3	7	1.01 USD/gallon (minimum selling price). Indirect heated entrained flow low pressure gasifier with lignocellulosic biomass as feedstock. Fixed bed reactor for alcohol synthesis and subsequent separation	1.23 USD/liter (average)	[115], [116], [117]

Table A.4: Gasification projects targeting interest chemicals

Company/Project	Country	Product	Feedstock	Status
Andritz/Bio2G	Sweden	SNG	Forest residues	Cancelled
Chemrec/Domsjö	Sweden	Methanol	Brown liquor	Cancelled
NextChem/Waste to Methanol	Italy	Methanol	Wastes	Study
GoBiGas	Sweden	SNG	Forest residues	Operating/ idling
Enerkem/Rotterdam	The Netherlands	Methanol	Wastes	Planning
Chemrec/Rottneros	Sweden	Methanol	Forest residues	Cancelled
Enerkem/Tarragona	Spain	Methanol	Wastes	Announced
Chemrec/Vallvik	Sweden	Methanol	Black liquor	Cancelled
Siemens/Woordspirit	The Netherlands	Methanol	Forest residues	Cancelled
TKI fka HTW/Värmlandsmetanol	Sweden	Methanol	Forest residues	Planning
Enerkem/Alberta Biofuels	Canada	Methanol/ Ethanol	RDF	Decommissioned
Ineos Bio	USA	Ethanol	Biomass wastes	Decommissioned
Enerkem/Pontotoc	USA	Ethanol	RDF	Cancelled
Range Fuel	USA	Methanol/ Ethanol	Forest residues	Decommissioned
InEnTec	USA	Ethanol	Orchard residues	Planned
Enerkem/Vanerco	Canada	Ethanol	RDF	Planned
Synova Power/Ambigo	The Netherlands	SNG	Biomass residues	On hold
Aichernig Engineering fka Repotec	France	SNG	Biomass residues	Operational
Chemrec/LTU Green Fuels	Sweden	Methanol/ DME	Black liquor	Idling
Adapted from [88]				

B

Appendix 2

Table B.1: WATER calculator block

Variable	Description	Fortran code
H2OIN	Compattr-Var (WETMSW) NC-MSW-PROXANAL-1	CONV = $\frac{\text{H2OIN - H2ODRY}}{100-\text{H2ODRY}}$ Before unit operation: DRIER
H2ODRY	Block-Var (DRYER) COMPATT NC-MSW-PROXANAL-1	
CONV	Block-Var (DRYER) CONV 1	

Table B.2: DECOMP calculator block

Variable	Description	Fortran
ULT	compattr-Vec (DRYMSW) NC - MSW - ULTANAL	C FACT IS THE FACTOR TO CONVERT THE ULTIMATE ANALYSIS TO A WET BASIS FACT = (100 - WATER) / 100 H2O = WATER / 100 ASH = ULT(1) / 100 * FACT CHAR = ULT(2) / 100 * FACT H2 = ULT(3) / 100 * FACT N2 = ULT(4) / 100 * FACT SULF = ULT(6) / 100 * FACT O2 = ULT(7) / 100 * FACT Before unit operation: DECOMP2
WATER	Compattr-Var (DRYMSW) NC-MSW-PROXANAL-1	
H2O	Block-Var (DECOMP2) MASS-YIELD H2O (MIXED)	
ASH	Block-Var (DECOMP2) MASS-YIELD ASH (NC)	
CHAR	Block-Var (DECOMP2) MASS-YIELD C (CI)	
H2	Block-Var (DECOMP2) MASS-YIELD H2 (MIXED)	
N2	Block-Var (DECOMP2) MASS-YIELD N2 (MIXED)	
SULF	Block-Var (DECOMP2) MASS-YIELD S (MIXED)	
O2	Block-Var (DECOMP2) MASS-YIELD O2 (MIXED)	

Table B.3: TARCONVE calculator block

Variable	Description	Fortran code
T	Import variable Stream-Var(GASIFOUT) MIXED Temp(C)	CONVERSION C –> TAR C Molar weights in kg/kmol MW1 = 94.11304 MW2 = 128.17352 MW3 = 92.14052 C SET THE TAR FORMATION in g/Nm3 dry TARn = 6.49 C Conversion factor (Nm3/kmol) FACT = 22.6831093254056 C VOLUME FLOW in Nm3 wet/hr (vs Nm3 dry /hr) VFLOW = MOLEFLOW * FACT VDRY = (MOLEFLOW - H2OMOLE) * FACT C TAR COMPOSITION C Linearisation(T) C Phenol (C6H6O) = COMPA C Naphthalene (C10H8) = COMPB C Toluene (C7H8) = COMPC COMPA = -0.0039 * T + 3.872 COMPB = -1E-5 * T + 0.002 COMPC = 0.0037 * T - 2.7833 C Adjust to a total composition of 1 ADJ = ((COMPA + COMPB + COMPC) -1)/3 COMP1 = COMPA - ADJ COMP2 = COMPB - ADJ COMP3 = COMPC - ADJ C INDIVIDUAL TAR FORMATION kg/Nm3 dry TAR1 = COMP1*TARN/1000 TAR2 = COMP2*TARN/1000 TAR3 = COMP3*TARN/1000 C MOLE FLOWS in kmol/hr (kg/Nm3 dry * Nm3 dry/hr / kg/kmol) NFLOW1 = TAR1*VDRY/MW1 NFLOW2 = TAR2*VDRY/MW2 NFLOW3 = TAR3*VDRY/MW3 C CONVERSIONS (EXPORT) C Reaction 4: 6C +3H2 + 0.5O2 -> C6H6O C Reaction 5: 10C + 4H2 -> C10H8 C Reaction 6: 7C + 4H2 -> C7H8 CONVTAR1 = 6*NFLOW1/CMOLE CONVTAR2 = 10*NFLOW2/CMOLE CONVTAR3 = 7*NFLOW3/CMOLE
H2OMOLE	Import variable Stream-var (GASIFOUT) MIXED H2O (kmol/h)	
CMOLE	Import variable Mole-Flow (PYRO-IN) CI C (kmol/h)	
FACT	Parameter: no=1	
VFLOW	Parameter: no=2	
VDRY	Parameter: no=3	
CONVTAR1	Export variable Block-Var (TARCONV) Conv-1-ID1=1	
CONVTAR2	Export variable Block-Var (TARCONV) Conv-1-ID1=2	
CONVTAR3	Export variable Block-Var (TARCONV) Conv-1-ID1=3	
COMP1	Parameter: no=4	
COMP2	Parameter: no=5	
COMP3	Parameter: no=6	
TAR1	Parameter: no=7	
TAR2	Parameter: no=8	
TAR3	Parameter: no=9	
NFLOW1	Parameter: no=10	
NFLOW2	Parameter: no=11	
NFLOW3	Parameter: no=12	

C
Appendix 3

Table C.1: AUTOTHER design spec

Variable	Description	Spec
QGASIF	Heat-Duty (QGASIF) MW MASS-FLOW (kg/sec)	QGASIF=0 Varying the mass flow of OXY (O_2, (kg/h)) injected in the combustion block between 1000 and 10000

Table C.2: STEAM design spec

Variable	Description	Spec
STEAMIN	Mass-Flow (STEAMM) MIXED H_2O (kg/h)	$\frac{\text{STEAMIN}}{\text{CHARIN+ASHIN}} = 0.8$ Varying the mass flow of STEAMIN (kg/h) between 1000 and 10000
CHARIN	Mass-Flow (PYROCHAR) CI C (kg/h)	
ASHIN	Mass-Flow (PYROCHAR) NC ASH (kg/h)	

Table C.3: RMEFLOW design spec

Variable	Description	Spec
MFLOWRME	Stream-Var (RME-IN) MIXED MASS-FLOW (kg/sec)	$\frac{\text{HHVRME}\cdot\text{MFLOWRME}}{\text{HHVSRCB2}\cdot\text{MFSCRUB2}} = 0.024$ Varying the mass flow of RME-IN (kg/sec) between 0.0001 and 10
MFSCRUB2	Stream-Var (TOSCRUB2) MIXED MASS-FLOW (kg/sec)	
HHVRME	Stream-Prop (RME-IN) HHV (J/kg)	
HHVSRCB2	Stream-Prop (RME-IN) HHV (J/kg) MASS-FLOW (kg/sec)	

Table C.4: Design spec for setting the desired H_2/CO ratio before the MeOH synthesis

Variable	Description	Spec
H2MOL	Mole-Flow (MIXOUT) MIXED H_2 (kmol/sec)	VALUE= 2.5 Varying the split flow fraction of the stream TOMIX in the block SPLIT between 0.1 and 1
COMOL	Mole-Flow (MIXOUT) MIXED CO (kmol/sec)	
VALUE	Parameter no.=1	

Table C.5: Design spec for the desired H_2O/CO ratio in the WGS reactor

Variable	Description	Spec
STEAMOL	Mole-Flow (HOTSTEAM) MIXED H_2O (kmol/sec)	VALUE= 1.5 Varying the H_2 molar flow of the HOTSTEAM stream between 0 and 1
COMOL	Mole-Flow (TOWGS) MIXED CO (kmol/sec)	
VALUE	Parameter no.=1)	

DEPARTMENT OF SOME SUBJECT OR TECHNOLOGY
CHALMERS UNIVERSITY OF TECHNOLOGY
Gothenburg, Sweden
www.chalmers.se

CHALMERS
UNIVERSITY OF TECHNOLOGY